Universidade de Lisboa

Faculdade de Farmácia

IDENTIFICATION AND CHARACTERIZATION OF HOST CATHEPSINS AND CYSTATINS DURING TUBERCULOSIS AND HIV CO-INFECTION OF ANTIGEN PRESENTING CELLS

Ana Catarina Arsénio Fialho

Dissertation supervised by Professor Elsa Anes and co-supervised by Professor José Miguel Azevedo Pereira.

Biopharmaceutical Sciences

2018

This work was partially financed by ADEIM and by the project FCT PTDC/SAU-INF/28182/2017

Abstract

The human immunodeficiency virus (HIV) infection and tuberculosis are still major health problems. It is estimated that one third of the human population is latently infected with tuberculosis, with HIV infection being the major risk for reactivation.

Eradication of HIV and *Mycobacterium tuberculosis* (Mtb) infections is challenging due to establishment of latent reservoirs, as is the case of macrophages (Mϕ) and dendritic cells (DC), and the emergence of drug resistant strains. This difficulty is aggravated during co-infection. Thus, there is the need to develop and establish an efficient treatment to eradicate these infections.

The long-term goal of this work is the development of a host-directed strategy that, through the manipulation of lysosomal proteases, will boost the host cellular and humoral response against these microorganisms.

In the first part of this thesis we performed a transcriptomic analysis of all cathepsins and their inhibitors cystatins during mono- or co-infections of Mϕ or DC. Upon co-infection with Mtb and HIV, DC and Mϕ have a differential profile of expression being the analysed genes upregulated and downregulated. Further, during co-infections, the gene expression was dominated by the HIV infection.

In the second part we explored the role of cathepsin S and their manipulation as a strategy to control Mtb infection. Study of the involvement of microRNAs, revealed that miR-106b-5p is manipulated by Mtb and that it reduces cathepsin S protein expression. Through loss-of-function experiments, cathepsin S expression, Mtb killing within Mϕ and T cell activation increased. The decrease of Mtb survival was independent of apoptosis, necrosis and autophagy suggesting that miR-106b-5p action on cathepsin S enables Mtb to evade to the degradative activity of enzymes of the endocytic pathway.

These results show a distinct expression profile between HIV Mtb co-infected DC and Mϕ and suggest cathepsin manipulation as a potential target for host directed therapy in Mtb infection.

Key-words: HIV, Mtb, co-infection, cathepsins, microRNAs

Resumo

O vírus da imunodeficiência humana (HIV) e a *Mycobacterium tuberculosis* (Mtb) são os patogenos causadores da síndrome da imunodeficiência adquirida e da tuberculose, respetivamente. É estimado que um terço da população mundial tem tuberculose latente, sendo a infeção por HIV o maior risco para a reactivação da tuberculose latente devido à extensa imunossupressão. A incidência da TB em pessoas infectadas por HIV teve um aumento de 40 % na Europa nos últimos 5 anos, sendo Portugal o terceiro país da Europa com a maior percentagem de pacientes com TB e infetados com HIV.

Embora as doenças causadas por HIV e por Mtb tenham vindo a ser extensivamente estudadas, ainda não existe uma terapia capaz de eliminar estas infeções. Estas dificuldades são causadas em parte pelo aparecimento de estirpes resistentes aos antibióticos/antivirais utilizados e pela existência de reservatórios celulares latentes que contêm estes patogenos num estado de dormência, permitindo que o sistema imune não os ataque nem que estes sejam alvos dos diversos tratamentos. Além disso, quando o mesmo hospedeiro é infetado por HIV e por Mtb a dificuldade em tratar e erradicar ambas as infeções é ainda mais crítica, dado que estes patogenos exacerbaram a infeção um do outro. Deste modo, é necessário desenvolver e estabelecer novos tratamentos de forma a erradicar ou atenuar cada mono-infeção ou co-infeção.

O objetivo deste projeto é o desenvolvimento de uma terapia direcionada ao hospedeiro, através da manipulação de proteases lisossomais, de forma a fortalecer a resposta celular e humoral do hospedeiro contra o HIV e o Mtb durante as mono-infeções e as co-infeções e potencialmente melhorar as terapias existentes. Para tal foi estabelecido um modelo de co-infeção que pretendia assemelhar-se à infeção por Mtb de um indíviduo previamente infectado por HIV e num estado de latência viral. Neste estudo foi também incluído um modelo de co-infeção por HIV-2 e Mtb. Desta forma foi estudada a infeção por HIV-2 que afecta um menor número de indivíduos comparativamente à infeção por HIV-1. Este vírus é também tido como um modelo de HIV com menor virulência.

Numa primeira fase, foi determinada a expressão genética das catepsinas e dos seus inibidores naturais, as cistatinas, durante a mono-infeção por Mtb, HIV-1 e HIV-2 e durante a co-infeção Mtb-HIV em células dendríticas e macrófagos. Numa segunda fase foi determinado se a manipulação da catepsina S por Mtb via

microRNAs (miRNAs) contribuía para a sobrevivência intracelular desta bactéria em macrófagos e para o escape à apresentação de antigénios a linfócitos T.

De forma a caracterizar o modelo de infeção estabelecido foi determinada a carga viral e micobacteriana das células assim como a morte celular das mesmas por apototse e necrose. A carga micobacteriana da mono-infeção por Mtb era superior à da co-infeção HIV Mtb em células dendríticas e macrófagos aquando da medição da expressão genética das catepsinas e cistatinas. A morte celular por apoptose e necrose foi também medida e revelou que enquanto as células dendríticas encontram-se maioritariamente num estado inicial de apoptose, os macrófagos apresentam uma maior percentagem de células em fases mais avançadas da apoptose. Em ambos os tipos celulares a necrose ocorre em menos de 1 % das células. Tanto as mono-infeções por HIV-1 e HIV-2 como as co-infeções tiveram um aumento na percentagem de células apoptóticas comparativamente com as mono-infeções com micobactéria, sugerindo que é o efeito do HIV que impera durante as co-infeções.

Neste trabalho foi elucidado o controlo da expressão genética resultante da infeção por Mtb, HIV-1 e HIV-2 durante a mono- e a co-infeção de células apresentadoras de antigénio. As células dendríticas e os macrófagos apresentam uma expressão genética diferencial entre si, observando-se um aumento de expressão geral nas células dendríticas relativamente a macrófagos. O perfil de expressão genética da mono-infeção por HIV-1 e por HIV-2 é idêntico em macrófagos, mas distinto em células dendríticas. Em ambos estes tipos celulares a expressão genética durante a co-infeção foi semelhante à da mono-infeção por HIV-1 e HIV-2. É de notar que as infeções bacterianas apresentam mais diferenças na expressão genética de catepsinas e cistatina durante a infeção de macrófagos. Em contraste, as infeções por HIV-1 e HIV-2 apresentam um maior número de genes diferencialmente expressos durante a infeção de células dendríticas.

O estudo do envolvimento dos microRNAs (miRNA) na modulação da resposta celular do hospedeiro após a infeção por Mtb em Mϕ mostrou que o miR-106b-5p é manipulado por este microrganismo. Sendo que este miRNA tem como alvo a catepsina S, uma das catepsinas que participa na degradação lisossomal do Mtb e na apresentação de antigénios, foi determinado o seu efeito na expressão desta proteína. Os resultados obtidos indicam que o miR-106b-5p reduz a expressão proteica da catepsina S. A manipulação deste miRNA permitiu observar que ao aumentar a sua expressão, a expressão da catepsina S diminui e a sobrevivência intracelular do Mtb aumenta. Em contraste, ao diminuir o miR-106b-5p houve o aumento da expressão da

catepsina S e a diminuição da sobrevivência intracelular do Mtb. Foi também demonstrado que a sobrevivência intracelular do Mtb é independente da apoptose, necrose e autofagia o que sugere que a ação do miR-106b-5p na catepsina S permite que o Mtb escape aos enzimas hidrolíticos das vias endocíticas. Ao inferir o impacto da manipulação do miR-106b-5p na apresentação de antigénios e consequentemente na ativação de células T, a inibição deste miRNA levou a um aumento da expressão de moléculas apresentadoras de antigénio à superfície da membrana celular dos Mϕ. Este aumento foi acompanhado por um aumento na ativação de células T após contacto com Mϕ infectados por Mtb.

Estes resultados mostram que existe uma expressão diferencial dos genes das catepsinas e cistatinas entre DC e Mϕ co-infectados com HIV-1 ou HIV-2 e Mtb e que o miR-106b-5p é um potencial alvo para o desenvolvimento de uma terapia direcionada durante a infeção por Mtb.

Palavras-chave: HIV, Mtb, co-infecção, catepsinas, microRNAs

Acknowledgements

This was until now the biggest and the most challenging project that I embraced.

I want to thank my supervisor, professor Elsa, and co-supervisor, professor José Miguel, for giving me the opportunity to develop this work, for answering my questions, for believing and guiding me.

A special thanks to David and Nuno for teaching me all the procedures, planning and troubleshooting related to our laboratory and to our precious mycobacteria. Among many things, you taught me that regardless of the time the sun rises, the day begins around 11am and that I must be prepared to be scared at any time! I also want to thank Marta, my HIV mentor, for initiating me in the P3, for telling me not to be afraid of a big volume of samples to process and how to handle that senior ultracentrifuge. To all of you a huge thanks for your patience, good mood, for clarifying all my doubts and for those conversations about both everything and nothing. Ricardo Calderón, thanks for your help in the laboratory.

A heartfelt thanks to Francisco, my colleague and friend, for helping me in the laboratory and life in general! I will never forget our P3 marathons. We still have to design and construct our *guiché*.

I´m very grateful for all the encouragement and care that my family gave me during this thesis and during all my life. This would not have been possible without them.

I would like to acknowledge *Instituto Português do Sangue e da Transplantação* and all the blood donors that unknowingly supported this thesis.

Finally, I acknowledge the opportunity to have participated in what follows:

- Pires, D. *et al. Mycobacterium tuberculosis* Modulates miR-106b-5p to Control Cathepsin S Expression Resulting in Higher Pathogen Survival and Poor T-Cell Activation. *Front. Immunol.* 8, 1–13 (2017).

- 10th iMed.ULisboa and 3nd i3du Postgraduate Students Meeting, Faculdade de Fármacia, Universidade de Lisboa, 2018, *HIV and Mycobaterium tuberculosis co-infection leads to a differential regulation of cathepsins and cystatins in macrophage and dendritic* cells

- 9th iMed.ULisboa and 2nd i3du Postgraduate Students Meeting, Faculdade de Fármacia, Universidade de Lisboa, 2017, *Inhibition of miR-106b-5p Improves the Antigen Presentation Capacity of Macrophages Infected with Mycobacteria*

- Science Talks, Tuberculose, Faculdade de Fármacia, Universidade de Lisboa, 2018, *Catepsinas, vias degradativas e o papel dos miRNA's e implicações no controlo da Tuberculose*

- 1º Simpósio de Investigação em Tuberculose e Micobactérias Não Tuberculosas em Portugal, Exploratório - Centro Ciência Viva de Coimbra, 2018

Index

Introduction

Mycobacterium tuberculosis (Mtb) and the human immunodeficiency virus (HIV) are the causative pathogens of tuberculosis (TB) and acquired immunodeficiency syndrome (AIDS), respectively. TB is the leading cause of death by an infectious agent and the 10th cause of death worldwide [1], registering 1.3 million death in 2016. It is estimated that 36.9 million people are currently living with HIV and that 1.8 million people became newly infected in 2017 [2]. In 2016, 1.2 million people were co-infected with Mtb and HIV, while 476 774 co-infected people died, with TB being the leading cause of death among HIV-infected individuals. Since TB in HIV-infected patients continues to grow, with an increase of 2 % in the number of TB patients with an HIV test result between 2015 to 2016, and with the increase of the cases with resistance to antibiotics and antivirals, it is crucial to develop other treatments that will enable to attenuate and eradicate these infections both during mono- and co-infection [1–4].

a. Route of transmission and propagation of infection

Mtb is mainly transmitted by the inhalation of airborne droplets containing the bacilli, expelled by an individual with active tuberculosis. Once inside the lungs of the new host, Mtb reaches the alveoli where it encounters resident alveolar Mϕ, DC and neutrophils, and may be readily eliminated by the innate immune response [5–7]. However, in 10 % of infection cases it resists to this response and persist in the lungs. While Mϕ differentiate to have a stronger effect *in situ*, DC mature to migrate to secondary lymphoid organs, prime naïve T cells and recruit more immune cells, particularly T cells and natural killer cells, to the infection site [5,6,8,9].

The recruitment of cells to the infection site leads to the formation of a granuloma, a structure composed of several layers of different types of cells and with a necrotic core, in which the bacilli is contained and may persist inside the host, establishing a latent infection [10]. This structure acts as a host defence, by impairing Mtb dissemination, however it can also serve as a replication niche for the mycobacteria[8]. When infection is not contained in the granuloma, bacteria will actively proliferate throughout the lung tissue, leading to active pulmonary tuberculosis, and to other organs and tissues, causing extrapulmonary tuberculosis [5,6,8,11].

HIV transmission occurs when body fluids of an infected person – blood, semen, breast milk, rectal and vaginal fluids – come into contact with damaged, mucosal membranes, e.g. the genital tract, or when directly introduced in the blood stream of an uninfected person [12]. Upon sexual transmission, HIV crosses the epithelial barriers of the mucosal membranes and its captured by epidermal Langerhans cells and other immune cells, such as Mϕ and DC, that try to contain HIV infection. Yet, virus replicates within the mucosa cells inducing the transference of virus from cell to cell, such as from Langerhans cells to mucosal T lymphocytes. The viral propagation may occur due to infection of cells by viral particles or by cell-to-cell infection, which is thought to be the preferential and most efficient way of viral spreading, due to a higher transfer of viral particles and proteins [13–15]. HIV infected T lymphocytes and DC then migrate to the lymph nodes, where viral replication continues, allowing dissemination of HIV into the bloodstream and consequently to several organs [16,17].

Thus, HIV infection is characterised by an initial acute stage, in which HIV rapidly replicates and spreads through the body, decreasing substantially the number of $CD4^+$ T cells. After this peak in HIV load, there is a significant reduction of HIV replication caused by the host immune response, and a slight increase in $CD4^+$ T cell counts. Afterwards, HIV infection enters in the asymptomatic stage, which can last for several years. This stage is characterized by low HIV loads and a gradual and irreversible reduction of $CD4^+$ T cells. Finally, after several years/decades, the immunodeficiency prevails, allowing the establishment of several opportunistic infections and cancers. This is the final stage of HIV infection: the AIDS stage [18–20].

b. HIV and Mtb escape from the immune system

Pathogen elimination is composed of an orchestra of cellular functions, such as phagocytosis, production of anti-microbial molecules, induction of inflammation, production of signalling molecules, apoptosis, among others. When cells are infected with HIV or Mtb, these pathogens manipulate their cellular mechanisms to survive and replicate within these cells.

As it was referred before, the response of the immune system to Mtb infection generally culminates with the formation of a **granuloma**, which is composed by several cell types, such as Mϕ, DC, T cells, foam cells and epithelial cells, with Mϕ being the primary cellular niches of Mtb. HIV preferentially infects $CD4^+$T cells and leads to their depletion, causing a decrease in the production of pro-inflammatory cytokines – interferon γ (IFN-γ), tumour necrosis factor α (TNF-α) – and interleukin 2 (IL-2), that

participate in T cell differentiation [21]. $CD4^+$T cells induce the activation of Mϕ and DC to enhance their antimicrobial effects with these cytokines, hence these lymphocytes are important for the maintenance of the granuloma [22]. Not only the generalized depletion of $CD4^+$T cells during HIV infection contributes to granuloma failure, but also HIV infection of Mϕ, DC and $CD4^+$T cells affects Mtb containment [23]. By infecting these cells, which are then recruited to the Mtb infection site, HIV as access to the interior of the granuloma where it replicates and further exacerbates TB [24,25].

These pathogens can tune **cellular receptors** to facilitate their entry in cells and to impair the immune response. Mtb infection may promote and facilitate HIV entry in cells since it can increase the expression of CXCR4 and CCR5, both co-receptors used by HIV to enter host cells, and decrease the levels of MIP-1β, the ligand for CCR5 and a blocker of HIV replication *in vitro*. In turn, HIV infection induces the expression of CD38, CD70, human leucocyte antigen DR (HLA-DR) that fragilizes T cell response against Mtb [24,26,27].

HIV and mycobacteria burden may be potentiated by cytokines and by HIV proteins. In HIV infected monocyte-derived macrophages (MDM) and in the chronically HIV infected monocytic U1 cell line, viral replication was shown to be enhanced by macrophage colony-stimulating factor (M-CSF), TNF-α, TNF-β, IFN-γ, IL-1, IL-4 and IL-6, and supressed by IFN-α, IFN-β, GM-CSF, IL-4, IL-10, IL-13 and IL-16 [21,27,28]. Mϕ activated by mycobacteria lipopolysaccharide (LPS) release TNF-α, IL-1 and IL-6, which were also shown to enhance viral replication and viral transcriptional activation during co-infection [24,29]. Co-infected MDM have a higher growth of Mtb then Mtb mono-infected MDM and stimuli with TNF-α and IFN-γ enhanced Mtb growth in MDM HIV infected but not in uninfected MDMs [28]. In contrast, Mtb growth is lower in HIV infected alveolar Mϕ with specific CD4 counts despite a higher ability of mycobacteria internalization and intracellular burden [30]. HIV proteins also contribute to enhancement of viral replication, especially Nef, Vpr and Tat, since they mimic TNF signalling and activate the HIV long terminal repeat (LTR) and the viral promoter [22,29,31].

Phagocytosis is a process by which particles, microorganisms, dead or dying cells are internalized and degraded within a phagolysosome. When pathogens are phagocytosed by phagocytic cells, such as DC and Mϕ, their degradation enables the presentation of pathogen-derived antigens that are presented at the surface of these cells to sensitize and activate other immune cells to fight infections. Briefly, particles are recognised by host cellular receptors triggering membrane remodelling and rearrangement of the actin cytoskeleton that allow the membrane to surround and

internalize the particles in a phagosome. Then this phagosome matures into a phagolysosome by fusion and fission with early, late endosomes and lysosomes, changing its content and membrane composition. In this process it becomes more acidic and acquires degradative enzymes, such as cathepsins, antimicrobial peptides, reactive oxygen species (ROS) and reactive nitrogen species (NOS), that confer it a degradative environment that enables degradation [32–34].

Mtb can prevent phagosome maturation by interfering with (i) phagosome acidification, (ii) membrane remodelling, through the inactivation of vesicular transport proteins -Ras-related protein-5 (Rab5) and Rab7; (iii) lysosome fusion, through the action of mycobacterial proteins, (iv) impairment of protein degradation, among others [35–40]. If Mtb cannot successfully inhibit phagosome maturation, it also has mechanism to resist to the phagolysosome environment [33,41,42].

HIV can trigger phagocytosis in infected and uninfected cells to impair the immune response. It interferes with Fcγ-mediated phagocytosis, through the downregulation of the expression of FcγR subunits, with endosome transport and actin polymerization, through the action of HIV proteins, such as Nef, Vif, Vpr, Tat and Rev [43–45].

When phagocytosis/endocytosis is blocked, **autophagy** can be initiated allowing pathogen degradation and elimination to continue. This process is based on the engulfment of cytoplasmic cargo, such as organelles or bacteria, in an autophagosome that then fuses with lysosomes allowing the degradation of their content [46]. Autophagy has been associated with programmed cell death. Its induction through IFN-γ, together with the production of NOS and antimicrobial peptides, are one of the cellular backup plans after phagocytosis/endocytosis failure. However Mtb and HIV may escape this pathway [21,47].

Mtb can inhibit autophagy through modulation of host proteins, as shown in the human leukaemia monocytic cell line (THP-1), due to the overexpression of the anti-autophagic factor Bfl-1/A1, and in mouse Mϕ [48,49]. Also, Mtb components and products, such as the lipoarabinomannan (LAM), were shown to inhibit autophagy in Mϕ, while for DC this was seen with the Esx-1 secretion system [50].

HIV inhibits autophagy through the action of Tat protein in monocytes and Mϕ by upregulating IL-10 and supressing IFN-γ-induced autophagy and by activating the Src-Akt and the STAT3 pathways known to inhibit this cellular process. When autophagy is blocked in early stages, Nef protein may lead to the accumulation of autophagosomes in Mϕ, consequently impairing autophagy [50].

By interfering with phagocytosis/endocytosis and autophagy, pathogens are also interfering with **antigen presentation.** These pathways degrade pathogens allowing the processing and delivery of pathogen-derived antigens to human leukocyte antigen (HLA) class II molecules. These molecules present antigens on the cellular membrane of the host infected cell and amplify the immune response by activating and expanding $CD4^+$T cells.

Mtb can interfere with antigen processing and presentation through TLR signalling, in part due to blockage of IFN-γ dependent induction of major histocompatibility complex (MHC) class II molecules. Mtb infected Mϕ were shown to have reduced expression of MHC class II molecules and decreased ability to present antigens, which may be due to the interaction of mycobacterial lipoproteins with the TLR2 receptor. These lipoproteins and cell wall glycolipids may act as agonists for this receptor enhancing the immune response, however the continuous TLR signalling, not only through TLR2 but also TLR4 and TLR9, may inhibit MHC class II antigen processing and presentation [51]. Besides TLR signalling, Mtb can also impair antigen presentation through the disruption of the endosomal sorting complex required for the transport of MHC class II molecules to the cellular membrane [52].

Antigen presentation by MHC class I and II molecules is also impaired during **HIV** infection. Expression of Nef decreases T cell stimulation efficiency and decreases surface expression of mature MHC class II molecules, leading to the accumulation of immature MHC class II molecules at the cellular surface [53]. Antigen presentation by MHC class I molecules to cytotoxic T cells may also be affected by Nef, since it interferes with transport of these molecules in the trans-Golgi network by interacting with host proteins related to this pathway [54].

Pathogen elimination can be accomplished through the induction of cell death. **Apoptosis** prevents the release of the content of the dying cell to the cellular environment, thus not inducing inflammation. It involves cell shrinkage, chromatin condensation, plasma membrane blebbing, disintegration of the nucleus and formation of apoptotic bodies. These apoptotic bodies are then phagocyted and degraded in the phagosome of phagocytic cells. Apoptosis can be activated through the extrinsic pathways by interactions of specific ligands with transmembrane death receptor, such as FasL/FasR, TNF-α/TNFR1 or TNFR2 and TRAIL/DR4 or DR5, or the intrinsic pathway by intracellular stimuli independent of receptors. Both of these pathways lead to the activation of caspases that in turn activate several other proteins that cause the cellular alterations referred previously [55].

Mtb can impair apoptosis and in turn induce necrosis, which is a type of cell death characterized by the loss of membrane integrity and induction of inflammation, thus promoting its dissemination. Mtb can escape apoptosis by inducing the dissociation of death receptors from the cellular membrane, neutralizing the antimicrobial activity of their ligands, by decreasing and increasing the expression of death receptors and anti-apoptotic proteins, respectively, among others [56–59].

During **HIV** infection, the virus may induce apoptosis of infected and uninfected cells to disseminate and impair the immune system. Its induction has been correlated with high expression levels of FasL in HIV infected monocytes, Mϕ and natural killer cells *in vivo*. HIV also increases the expression levels of TRAIL in DC and Mϕ, thus mediating apoptosis of uninfected and infected cells [60,61]. HIV proteins have a crucial role during balance of apoptosis, having an anti- or pro-apoptotic effect by up and downregulating anti-apoptotic proteins, death cell receptors and ligands, preventing caspase activation, among others [31,60,62–64].

c. Cathepsins and cystatins as players of the immune system

A group of important players in the destruction of pathogens inside infected cells are acidic hydrolytic lysosomal enzymes. Lysosomes are known to contain a degradative environment not only due to the acid pH, ROS and NOS but also due to enzymes that are capable of degrading polysaccharides, nucleotides, lipids, peptides, among other.

Proteases are responsible for the hydrolysis of peptide bounds and can be classified according to their catalytic target in metalloproteases, aspartic, cysteine, serine and threonine proteases, being these the classes that are present in human cells although there are more. Among proteases, human cells express 15 cathepsins: two aspartic proteases – cathepsin D and E –, two serine proteases – cathepsin A and G -, and the remain are cysteine proteases – cathepsin B, C, F, H, K, L, O, S, V, W and Z. These can have endopeptidase activity – cathepsin D, E, F, G, K, L, S and V-, exopeptidase activity- cathepsin A, C and Z – or both – cathepsin B and H [65,66].

The expression and localization of each cathepsin is associated with their function. Hence, cathepsin B, C, D, F, H, L, V, Z are ubiquitously expressed, while cathepsin K, L, S and W are tissue-specific [67]. These proteases can be contained in the lysosome and endosomes or be secreted for the extracellular space enabling them to participate (i) in TLR signalling, as does cathepsin B and F, which were shown to be

required for the proteolytic cleavage of TLR7 and TLR9; (ii) in cytokine release and receptor activation, as shown by cathepsin G and its relationship with IL-1β, IL-8, TNF-α and the epidermal growth factor receptor; (iii) in the remodelling of the extracellular matrix, e.g. cathepsin K degrades collagen due to its collagenase activity; (iv) in antigen processing, by degrading extracellular proteins from internalized pathogens, and antigen presentation at the level of the MHC class II, by dissociating the invariant chain of these receptors and leading to their maturation, e.g. cathepsin L and S; (v) T cell migration, e.g. cathepsin Z; and also (vi) in apoptosis, as seen for cathepsin D, which activates caspase-8 in neutrophils, and cathepsin B that, by cleaving Bid, a pro-apoptotic protein, induces caspase activation and so apoptosis in neutrophils [65,68,69].

Since cathepsins catalyse the irreversible hydrolysis of peptide bonds, they are tightly regulated during their transcription, activation and activity. Cathepsins are synthetized in the cell cytoplasm as inactive enzymes and, after post-translational modifications in the endoplasmic reticulum, they are sorted to the Golgi network. They are then incorporated in endosomes and delivered to lysosomes, becoming activated by the action of other proteases or by autocatalysis promoted by the acidic environment. Their activity is manly regulated by their endogenous inhibitors - cystatins, stefins, thyropins and serpins. Cathepsins are known to be inhibited by several cystatins, such as cystatin A, B, C, D, E/M, F and SN. These inhibitors bind reversibly to these proteases in their active site, thus competing with the substrate [70–72].

These proteins and their regulators are important elements of the immune system. Defects and dysregulation of cathepsins caused by mutations, increased expression or activity, can be associated with cancer, Alzheimer's, obesity, inflammatory disease, genetic disorders, like the hereditary cystatin-C amyloid angiopathy, Mtb and HIV infections, and so on [73,74].

d. MicroRNAs as tools for host directed therapy

MicroRNAs (miRNAs) are non-coding RNA sequences with around 21-24 nucleotides that regulate post-transcriptional gene expression [75]. These molecules target specific mRNAs when incorporated in the RNA-induced silencing complex and upon binding to their targets they lead to inhibition of mRNA translation or degradation [76].

MicroRNAs can regulate the development and function of innate and adaptive immune cells and their dysregulation was shown to occur in several cancers and

autoimmune diseases where immune response is compromised [77]. In the context of bacterial or viral infections, not only miRNAs serve as a host cellular defence as their manipulation by the pathogens may confer them intracellular advantages, such as modulation of the inflammatory response [78]. In Mtb infection several miRNAs have been described to be dysregulated and to be manipulated by this pathogen, such as miR-142-3p [79], leading to impaired phagocytosis, chemotaxis, cytokine signalling and apotosis [80]. For HIV infection it has been proposed that some viral proteins directly interact with or alter the expression of proteins that participate in the biogenesis and maturation of miRNAs. In turn, some miRNAs were shown to have anti-HIV activity by binding to viral mRNA, such as miR-223, while others enhanced HIV infection, such as miR-132 [81].

The increasing appearance of Mtb and HIV drug-resistant strains and the existence of latent cell reservoirs are severe obstacles for HIV eradication and Mtb control and has boosted the development of new therapeutics. miRNAs mimics or inhibitors might serve as post-transcriptional regulators of several host factors that intervene in the infection. Thus, modulation of miRNAs can contribute to the development of novel treatments that are not restrained to drug resistance and to the replication status of the pathogen [75,82].

Objective

HIV and Mtb can impair cathepsin-related functions, such as antigen presentation, phagosome maturation and pathogen degradation. With the general aim of developing a host directed therapy this thesis has two main goals: (i) decipher the expression profile of cathepsins and cystatins during Mtb, HIV-1 and HIV-2 mono-infections and during HIV Mtb co-infection of monocyte-derived macrophages and dendritic cells; (ii) to gain control over Mtb infection by modulating lysosomal hydrolases expression through the manipulation of miRNAs in monocyte-derived macrophages mono-infected with Mtb.

Materials and Methods

Cell lines and culture conditions

Total PBMCs, $CD4^+$ lymphocytes and $CD14^+$ monocytes were isolated from buffy coats from healthy donors provided by the national blood institute (Instituto Português do Sangue, Lisbon, Portugal). $CD14^+$ monocytes were differentiated into dendritic cells (DC) or macrophages (Mϕ).

Buffy coats were diluted ½ with MACS buffer (EDTA 2 mM Gibco, 0.5 % inactivated fetal bovine serum (FBS) Corning, phosphate-buffered saline (PBS) without Ca^{2+} and Mg^{2+} pH 7.2 Gibco) and its components were separated with a density gradient centrifugation (800 x *g*, 20 min) using Ficoll-Paque (GE Healthcare Life Science). This gradient leads to the formation of a top layer of plasma, a second layer where PBMCs and lymphocytes are found, a third layer of Ficoll-Paque and a last and most dense layer composed of erythrocytes. The second layer was recovered, the cells were resuspended in MACS buffer, and centrifuged at 500 *g* for 10 min. The resulting supernatant was rejected. Cells were resuspended in MACS buffer, centrifuged (500 x *g*, 5 min) and the resulting cell pellet was resuspended in MACS buffer. $CD14^+$ and $CD4^+$ cells were isolated by incubation of the resuspended pellet in Micromagnetic beads $CD14^+$ (Miltenyi Biotec) and Micromagnetic beads $CD4^+$ T cell isolation kit, respectively. Cells were separated with MACS cell separation system following the manufacturer instructions (Miltenyi Biotec).

After separation, $CD14^+$ cells and $CD4^+$ cells were counted, centrifuged at 500 x *g* for 5 min, resuspended in the appropriate volume medium and seeded as needed. $CD4^+$ cells were resuspended in RPMI 1640 medium (Gibco) with 15 % FBS (Corning), 1 % L-glutamine 200 mM (HyClone), 50 µg/mL gentamicin (Gibco), 20 U/mL IL-2 and 3 µg/mL polybrene (Sigma). $CD14^+$ cells were differentiated in DC and Mϕ for 7 days and in the 4^{th} day of differentiation fresh media supplemented with the respective cytokines was added. For DC differentiation, $CD14^+$ cells were seeded in RPMI complete medium - RPMI medium containing 10 % FBS (Corning), 1 % sodium pyruvate (HyClone), 1 % penincillin streptomycin (Gibco), 1 % glutaMAX (Gibco), 1 % HEPES buffer (HyClone), 0.1 % β-mercaptoethanol (Gibco) – with granulocyte-macrophage colony-stimulating factor (GM-CSF) 10 ng/mL and interleukin 4 (IL-4) 20ng/mL (ImmunoTools). For Mϕ differentiation, $CD14^+$ cells were cultured for 3 h in RPMI medium (Gibco) containing 1 % glutaMAX (Gibco) and 1 % HEPES buffer (HyClone). Afterwards it was added medium containing 20 % FBS (Corning), 2 % sodium pyruvate (HyClone), 2 % penincillin streptomycin (Gibco), 2 % glutaMAX (Gibco), 2 % HEPES buffer (HyClone), 0.2 % β-mercaptoethanol (Gibco) and macrophage colony-stimulating factor 20 ng/mL (M-CSF) (ImmunoTools).

Mycobacterium smegmatis mc^2 155, containing a p19 (long lived) EGFP plasmid (Msm-GFP), the green fluorescent protein (GFP)-expressing strain of *Mycobacterium tuberculosis* (H37Rv-pEGFP) plasmid (Mtb-GFP), the *Mycobacterium smegmatis* mc2155 wild type strain (Msm) and the *Mycobacterium tuberculosis* H37Rv strain (Mtb) are part of the mycobacteria library of our research unit (Host-Pathogen Interaction Unit, at iMed.ULisboa). Msm strains were grown in medium containing Middlebrook's

7H9 Medium (Difco), nutrient broth (Difco) supplemented with 0.5 % glucose (Sigma) and 0.05 % Tween 80 (Sigma) at 37 °C on a shaker at 200 r.p.m. Mtb strains were grown in Middlebrook's 7H9 medium supplemented with 5 % glycerol (Invitrogen), 0.05 % (v/v) Tween 80 (Sigma) and 10 % OADC Enrichment (Difco) at 37 °C, 5 % CO_2.

HIV-1 92US660 (biotype R5) and HIV-2 Cas.04 (biotype R5X4R8) isolates were previously obtained from infected patients' and are part of the HIV library of our research unit (Host-Pathogen Interaction Unit, at iMed.ULisboa). New viral stocks of these virus were established in phytohaemagglutinin (PHA) stimulated PBMCs, which were isolated from buffy coats from healthy donors provided by the national blood institute (Instituto Português do Sangue, Lisbon, Portugal). Buffy coats were processed as described previously. The resultant cell pellet was resuspended in RPMI media containing 15 % FBS (Corning), 50 µg/mL gentamicin (Gibco), 1 % L-glutamine 20 mM (Hyclone) and 3 µg/mL PHA (Sigma). Cells were counted, seeded and stimulated for 3 days with PHA. After this period, cells were counted and resuspended in RPMI medium containing 15 % FBS (Corning), 50 µg/mL gentamicin (Gibco), 1 % L-glutamine 20 mM (HyClone), 20 U/mL IL-2 (ImmunoTools) and 3 µg/mL polybrene (Sigma). -80 ºC frozen aliquots of the viruses with high viral load were thawed at 37ºC and added to the PHA stimulated PBMCs. At day 7, 14, 20 and 28, PHA stimulated PBMCs were added to the viral cultures and the volume was adjusted with medium. Virus production was measured at day 10, 18 and 22 with an enzyme immunoassay (INNOTEST HIV Antigen mAb, Fujirebio) that detects the presence of p24 protein of HIV-1 and HIV-2. On day 30, the viral supernatant of cells was stored at -80 ºC, being the viral replication assessed by measuring the activity of the viral reverse transcriptase enzyme using Lenti RT Activity Kit (CAVIDI).

Infections of DC, Mϕ and PBMCs

Viral stocks were ultracentrifuged for 1 h at 50 000 x *g* and resuspended in the appropriate volume of RPMI complete medium. 7 days differentiated DC and Mϕ were centrifuged for 5 min at 500 *g*, the culture medium was removed and cells were infected with RPMI complete medium containing 1ng of HIV-1 or HIV-2 reverse transcriptase (RT) per 9 x 10^5 cells for 24 h at 37 ºC, in 5 %CO_2.

Mycobacteria cultures on exponential growth phase (Msm, Msm-GFP, Mtb or Mtb-GFP) were centrifuged (3000 x *g*, 5 min), washed in PBS (Gibco), centrifuged again (3000 x *g*, 5 min), resuspended in RPMI complete medium without antibiotics and subjected to an ultrasonic bath. Further centrifugation (500 x g, 1 min) and absorbance readings at 600 nm allowed to determine bacteria optical density. Cells were washed with PBS and incubated with mycobacteria at MOI 1 (1 bacteria/cell) for 3 h at 37 ºC, in 5 % CO_2. After this period RPMI complete medium without penincilin-spreptomycin (Gibco) and 5µg/mL gentamicin (Gibco) was added and cells were incubated for the desired time at 37 ºC, in 5 % CO_2.

For the co-infection, cells were first infected with the virus for 24 h, following infection with mycobacteria for 3 h and maintained in culture until 48 h after bacterial infection.

The following conditions were studied: no infection, Msm, Mtb, HIV-1 or HIV-2 mono-infection and HIV-1 Msm, HIV-2 Msm, HIV-1 Mtb or HIV-2 Mtb co-infection.

HIV replication

DC, Mϕ and PBMCs were seeded in 12-well plates at a density of 9 x 10^5 cells/well. Supernatant of infected cells was collected 72 h after the HIV-1 or HIV-2 infection, centrifuged (500 x *g*, 5 min) to remove any cells and then viral replication was analysed using Lenti RT Activity Kit (CAVIDI). This assay detects the activity of the viral reverse transcriptase being a measure for viral replication. Briefly, the RT present in the sample synthetizes a DNA strand from the RNA template provided using BrdUTP labelled nucleotides. The labelled DNA strand is then detected with an alkaline phosphatase conjugated α-BrdU antibody and a colorimetric alkaline phosphatase substrate, being the activity of this enzyme proportional to the RT activity. Infection of PBMCs was used as positive control.

HIV integration

DC, Mϕ and PBMCs were seeded in 12-well plates at a density of 9 x 10^5 cells/well. Following infection, DNA was extracted using the NZY Tissue gDNA Isolation kit (NZYTech). Cells were treated with proteinase K and RNase A, to remove proteins and RNA, lysed and applied in a silica-based spin column with affinity to DNA. After several rounds of washing and centrifugation steps, DNA was eluted. The quantity and quality of the DNA was determined by measuring the 260/230 and 260/280 nm absorbance ratios using a NanoDrop™ 1000 spectrophotometer.

DNA was amplified by nested PCR using the NZYTaq II 2× Green Master Mix (NZYTech) and a specific set of primers that bind to *Alu* sequences, the long terminal repeat (LTR) or the *gag* gene - Table 1. The PCR conditions used are shown in Table 2. DNA amplification fragments were separated by a 2 % agarose gel electrophoresis and were visualized with ethidium bromide (2.07 ng/mL) in a transilluminator. The 100 bp DNA ladder (New England Biolabs) was used to determine the size of the DNA bands.

Table 1: Description of the primers used in the amplification of HIV DNA. For each viral strain it was used two pair of primers designed to bind to an *Alu* sequence, the LTR or the *gag* gene. Forward and reverse primers are denotated with an F or R superscript, respectively.

Virus type	PCR	DNA primer binding site	Primer sequence	Expected fragment size / bp
HIV-1	1º	Alu ^{F}	TCC CAG CTA CTG GGG AGG CTG AGG	-
		LTR ^{R}	AGG CAA GCT TTA TTG AGG CTT AAG C	
	2º	LTR ^{F}	CTG TGG ATC TAC CAC ACA CAA GGC TAC	391
		LTR ^{R}	GCT GCT TAT ATG TAG CAT CTG AGG GC	
HIV-2	1º	Alu ^{F}	TCC CAG CTA CTG GGG AGG CTG AGG	-
		gag ^{R}	CAT AGG GCG TGC AGC CTT C	
	2º	*gag* ^{F}	GGC GGC AGG AAC AAA CCA	508
		gag ^{R}	TTC TGC CGC TAG ATG TCT C	

Table 2: PCR conditions for HIV DNA amplification. PCR conditions took into consideration the recommendations of the NZYTaq II 2× Green Master Mix (NZYTech) and the annealing temperature of each pair of primers: (*) first PCR - HIV-1 50 ºC, HIV-2 53 ºC; second PCR - HIV-1 50 ºC, HIV-2 62.5 ºC.

Cycle step	Temperature /°C	Time /s	Number of cycles
Initial denaturation	95	120	1
Denaturation	95	30	35
Annealing	*	30	
Extension	72	60s/kb	
Final Extension	72	600	1

RNA extraction

DC and Mϕ were seeded in 12-well plates at a density of 9 x 10^5 cells/well. After infection, RNA was extracted using the NZY Total RNA Isolation kit (NZYTech) following manufacturer instructions. RNA bounded to the silica membrane column was eluted and its quantity and quality was determined by measuring the 260/230 and 260/280 nm absorbance ratios using a NanoDrop™ 1000 spectrophotometer.

For microRNA experiments, Mø were seeded in 6-well plates at a density of 2 x 10^6 cells/well. RNA was isolated and purified from infected cells using Trizol reagent (Invitrogen) following the manufacturer protocol.

Real-time polymerase chain reaction

cDNA was synthetized from cellular RNA using the NZY First-Strand cDNA Synthesis Kit (NZYTech) following the kit instructions. This cDNA was then added to the NZY qPCR Green Master Mix (2x), ROX (NZYTech) in optimized conditions (final volume of the reaction mix of 5µL: 2.5 µL of NZY qPCR Green Master Mix (2x), ROX, primers to a final concentration of 10µM, 1.5 µL cDNA, 0.5 µL nuclease-free water) following the PCR conditions of the manufacturer. Real-time PCR was performed in a QuantStudio™ 7 Flex System (ThermoFischer). Gene expression was analysed using the $^{\Delta\Delta}$Ct method and glyceraldehyde 3-phosphate dehydrogenase (GAPDH) as the reference gene. Primers sequence is shown in Annex Table 1. For each condition, three biological replicates were tested. For every biological replicate, two technical replicates were performed.

The relative quantification of miRNAs in total RNA samples was performed by Exiqon (DK) miRNA qPCR services on RNA purified samples in triplicate. The specific quantification of miR-106b-5p in total RNA samples was performed in our laboratory using miRCURY LNA™ Universal RT miRNA PCR system (Exiqon) according to the manufacturer protocol and using the Exiqon LNA™ PCR primer sets: hsa-miR-106b-5p (205884), hsa-miR-23a-3p (204772), hsa-miR-23b-3p (204790), and hsa-miR-24-3p (204260). The qPCR was performed using an ABI 7300 Real Time PCR. The reaction

proceeded as follows: 1 cycle of 95 °C for 10 min, followed by 40 cycles of 95 °C for 10 s and 60 °C for 1 min. The miRNA expression profiles were normalized to the average obtained between miR-23a, miR-23b, and miR-24.

Transfection

Transfection of Mϕ with anti-cathepsin S siRNA or with miR-106b-5p mimics and inhibitors was performed with Biontex K2® Transfection System. Cells were incubated for 2 h with 4 µL/mL of K2 Multiplier reagent in culture medium, then incubated for 24 h with the transfection reagent and 100 nM of SMARTpool ON-TARGETplus human CTS S siRNA or with miRIDIAN miRNA human hsa-miR-106b-5p mimics or hairpin inhibitors and the respective siRNA or miRNA non-targeting controls (GE Dharmacon) in a ratio of 5 µL reagent: 1 µg siRNA in antibiotic-free medium. Afterwards, transfection medium was removed, and the cells were incubated for 3 days in fresh medium prior to any experiment.

Western Blot

Mø were seeded in 6-well plates at a density of 2 x 10^6 cells/well. Total proteins were recovered with 200 µL of Laemmli buffer (Sigma-Aldrich). Protein extracts were subjected to electrophoresis in 12 % SDS-PAGE gels and were transferred from the polyacrylamide gel to a nitrocellulose membrane by wet transfer using the Mini-PROTEAN tetra electrophoresis system (Bio-Rad). The nitrocellulose membrane was blocked in Tris-buffered saline with 0.1 % Tween 20 and 5 % of bovine serum albumin (BSA). The nitrocellulose membranes were incubated with primary antibodies specific for human cathepsin S and β-tubulin (Abcam, 92780 and 6046, respectively), overnight at 4 °C. All membranes were washed and incubated with secondary HRP-conjugated antibodies (Biorad). The bands were visualized with Luminata Crescendo Western HRP substrate (Merck Millipore) and quantified using ImageJ.

Immunofluorescence

Mø were seeded in 24-well plates at a density of 3 x 10^5 cells/well. Following the experiments, the samples were fixed with 4 % paraformaldehyde in PBS (Gibco) for 1 h and quenched by incubating with PBS 50 mM NH_4Cl. Mϕ were permeabilized with 0.1 % Triton in PBS for 5 min, washed and blocked with 1 % BSA (Merck Millipore) in PBS. Cells were stained with anti-LC3b antibody (Cell Signaling, 2775) in 1 % BSA in PBS overnight at room temperature. Following that, the cell nuclei were stained with 5 µg/ml of Hoechst dye (Thermo Scientific) for 10 min. Samples were mounted with ProLong™ Gold antifade mountant and analyzed by confocal microscopy (Leica AOBS SP5).

Flow cytometry

DC and Mϕ were seeded in 96-well plates at a density of 5 x 10^4 cells/well. Following mono or co-infected with HIV and mycobacteria, apoptosis and necrosis were measured using the PE Annexin V Apoptosis Detection Kit with 7-AAD (BioLegend). Cells were detached from the wells using Accutase (Corning), washed, incubated with annexin V and 7-AAD staining solutions as stated in the kit instructions, fixed with 4 % paraformaldehyde for 30 min.

For microRNA experiments, Mø were seeded in 24-well plates at a density of 3 x 10^5 cells per well. Following the experiment, cells were recovered with 5 mM EDTA (Gibco)/PBS solution, fixed with 4 % paraformaldehyde for 1 h and stained for 30 min with antibodies specific for human HLA-DR (clone L243, Biolegend), CD14, CD4 (BD Biosciences), or Annexin V and propidium iodide (Immonotools, GmbH) for the quantification of apoptotic and necrotic cells.

All samples were analysed in Guava easyCyte™5HT flow cytometer.

CD4 Proliferation

Mø were seeded in 48-well plates at a density of 1.5 x 10^5 cells/well. After 24 h of infection with Mtb CD4 lymphocytes were added to the culture at a ratio of 5 lymphocytes per Mø. CD4 lymphocytes were recovered after 5 days of coculture and quantified using Guava easyCyte™ 5HT flow cytometer.

Mycobacteria intracellular survival

Mϕ were seeded in 96-well plates at a density of 5 x 10^4 cells/well and infected with Mtb as previously described. After 3 h, 1, 3 and 5 days of infection Mϕ were lysed in 0,05 % Igepal (Sigma). Serial dilutions of the resulting bacterial suspensions were plated in Middlebrook 7H10 with 10 % OADC (Difco) and incubated for 2–3 weeks at 37 °C before colonies were observable.

Statistical Analysis

Data is presented as mean with the respective standard deviation or standard error (referred when used). Statistical analysis was performed with SigmaPlot 11. Multiple comparisons were made using one-way ANOVA followed by pairwise comparisons of the groups using Holm-Sidak test. Two group comparisons were made using Student's t-test. The considered nominal alpha criterion level was 0.05 below which differences between samples were deemed significant (*$p<0.05$; **$p<0.01$; ***$p<0.001$; # $p=0.001$).

Results

1. Characterization of the infection

To study HIV Mtb co-infection, it was established an experimental model that would resemble a sequence of events in which dendritic cells (DC) and macrophages (Mϕ) of an HIV-infected individual would be infected with Mtb. For that, cells were firstly challenged with HIV for 24 h, then with Mtb for 3h and were analysed 48 h after mycobacterium internalization into cells. This allowed time for the HIV infection to establish and then for the Mtb infection to produce visible results in gene manipulation.

Besides HIV-1 Mtb co-infection model it was also established a HIV-2 Mtb co-infection model. Individuals infected by HIV-2 typically display low viral loads and slower progression of the infection to AIDS comparatively to HIV-1 infected patients. Thus, HIV-2 is considered a less virulent model of HIV infection [83].

DC and Mϕ are not the primary replication niches of HIV and are also viral reservoirs therefore we used HIV-1 92US660 and HIV-2 Cas.04 (clinical isolates), which are non-replicative virus in these phagocytes, to mimic viral latency in these cells. *Mycobacterium smegmatis* (Msm) was used as control, since cells infected by this species efficiently eliminate infection.

Since the main objective is to study the impact of HIV and Mtb co-infection on DC and Mϕ cathepsin and cystatin gene expression, the co-infection model was characterized. It was determined if the infection had been established, the HIV and Mtb burden and the impact of each infection in cell viability at the time of gene expression analysis.

HIV is a retrovirus and since one of the steps of its replication cycle is the integration of the viral DNA in the host genome, viral infection was confirmed by nested polymerase chain reaction (PCR). The first PCR amplifies a region comprising an *Alu* sequence and the viral LTR or the *gag* gene. From the product of this reaction, a second PCR amplifies HIV-specific nucleotide sequence, for HIV-1 the viral LTR and for HIV-2 the *gag* gene.

To detect viral integration at the time of gene expression evaluation, DC and Mϕ were infected with HIV-1 or HIV-2 for 24 h. DNA extraction was performed after an additional 48 h and amplification products from nested PCR were visualized by electrophoresis with ethidium bromide. Integration of HIV-1 genome is confirmed by the appearance of a band with 391 base pairs corresponding to the LTR region. HIV-2 integration is confirmed by a band with 508 base pairs corresponding to a region of the *gag* gene. Peripheral blood mononuclear cells (PBMC) were used as positive controls since these cells are productively infected with both HIV-1 and HIV-2.

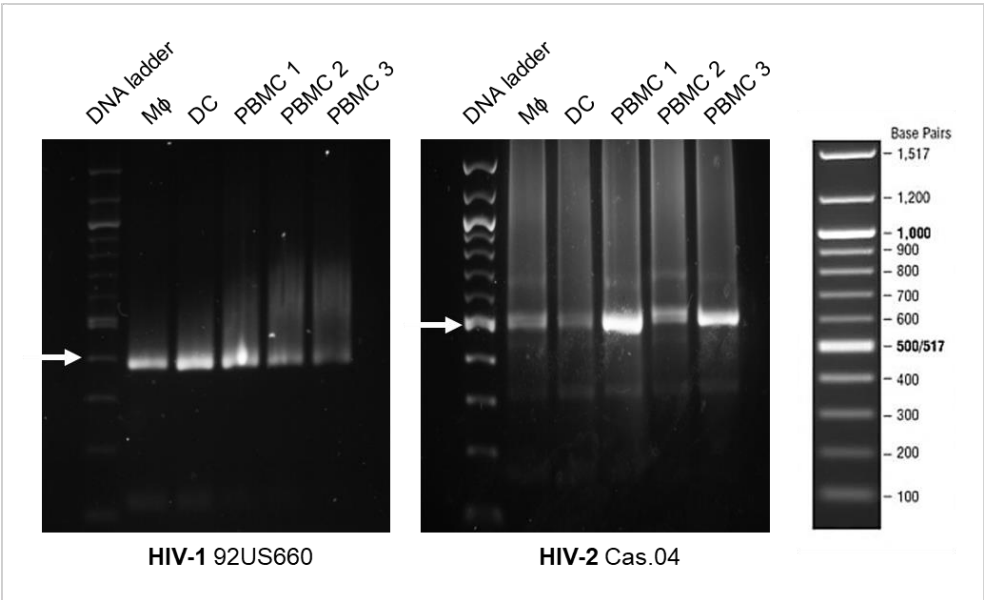

Figure 1: HIV-1 and HIV-2 integrate in the host cell genome. PBMCs, DC and Mϕ were infected with HIV-1 or HIV-2 for 24 h and DNA extraction was performed 72 h postinfection. For all samples, viral integration was determined from a template of 50 ng of DNA. Amplification of HIV-1 (92US660) LTR and HIV-2 (Cas.04) *gag* gene leads to the formation of an amplicon with 391 base pairs (bp) and 508 bp, respectively. The DNA ladder (New England Biolabs) is shown in the right side of the figure. White arrows indicate the DNA ladder band with the closest bp size of the amplicon: 400 bp for HIV-1 and 500 bp for HIV-2. PBMCs 1, 2 and 3 are biological replicates.

As seen in Figure 1, a band with less than 400 bp is detected in Mϕ, DC and PBMC infected with HIV-1 and a band with around 500 bp is detected in all these cell types when infected with HIV-2. These bands result from the amplification of the viral LTR and the *gag* gene and allow to conclude that these cells were infected with HIV and that viral integration occurred. It is also observed a difference in the intensity of the bands. For HIV-1 infected Mϕ, DC and PBMC 1, the band intensity is similar and higher than for PBMC 2 and 3. For HIV-2 infection, PBMC 1 and 3 bands have higher intensity

comparatively to the remaining samples and PBMC 2 as a higher intensity than Mϕ and DC.

During HIV replication cycle the viral RNA is retrotranscribed to double stranded DNA and integrated in the host cell genome. This is achieved by the activity of the reverse transcriptase (RT) enzyme. By measuring the activity of this enzyme in cellular supernatant, it can be inferred if the virus is propagating within cells since RT production is also associated with virions. HIV-1 92US660 and HIV-2 Cas.04 were previously shown by our lab team to be non-replicative virus in both Mϕ and DC (un-published results), so viral replication was measured not only to confirm these results during mono-infection but also to infer if the mycobacterium infection would alter HIV replication.

Mϕ and DC were infected as previously described for viral integration. Cell supernatant was collected 48 h after mycobacteria infection and RT activity was measured by enzyme-linked immunoassay. This supernatant was collected from the same cells for which the gene expression of cathepsins and cystatins was measured.

HIV-1 and HIV-2 mono-infections of Mϕ and DC didn't show any RT activity comparatively to infected PBMCs, which was in accordance with the previous results from our team. During co-infection with mycobacteria, RT activity was not detected (Annex Table 2). Thus, infection of DC and Mϕ with HIV-1 92US660 and HIV-2 Cas.04 is non-productive both in viral mono-infections and co-infections with Msm or Mtb.

As to determine mycobacteria burden at the time of cathepsins and cystatins gene expression measurement, DC and Mϕ were mono- and co-infected with HIV-1 or HIV-2 and *Mycobacterium spp* strains expressing a GFP plasmid, Msm-GFP or Mtb-GPF. The percentage of GFP positive cells was measured by flow cytometry 48 h after bacteria internalization.

When comparing both cells types, Mϕ have a higher burden in all infections comparatively to DC, and within the same cell type it is observed that Msm mono- and co-infections have a lower bacterial burden than Mtb infections (Figure 2).

Among infections and for DC and Mϕ, the lowest percentage of *Mycobacterium spp* infected cells is displayed during Msm mono-infection, while the highest is observed during Mtb mono-infections. In both cell types, Msm co-infections have a higher percentage of bacteria infected cells comparatively to mono-infection, whereas

Mtb co-infections have a lower percentage in comparison with Mtb mono-infection (Figure 2).

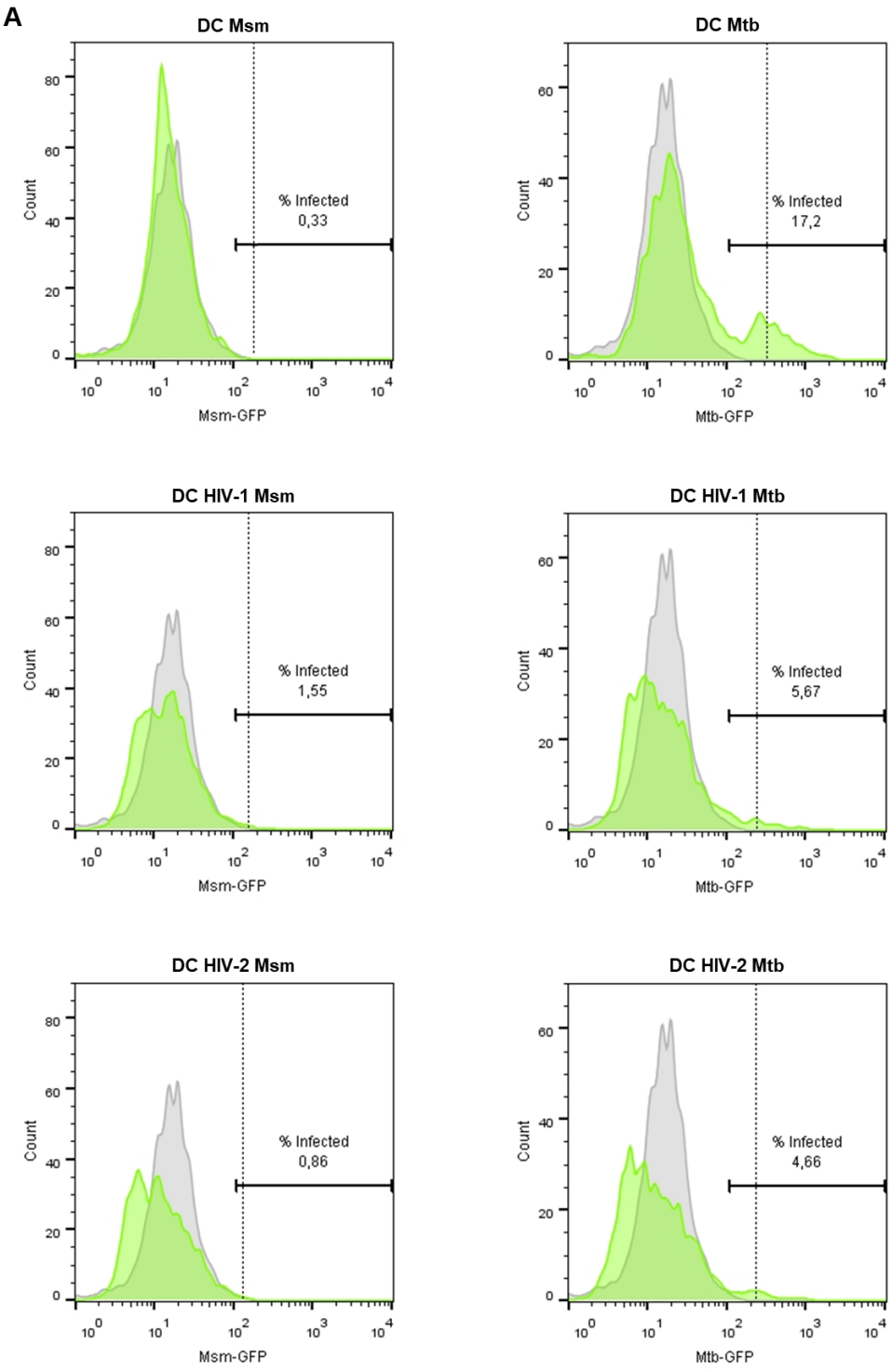

Figure 2: Continued

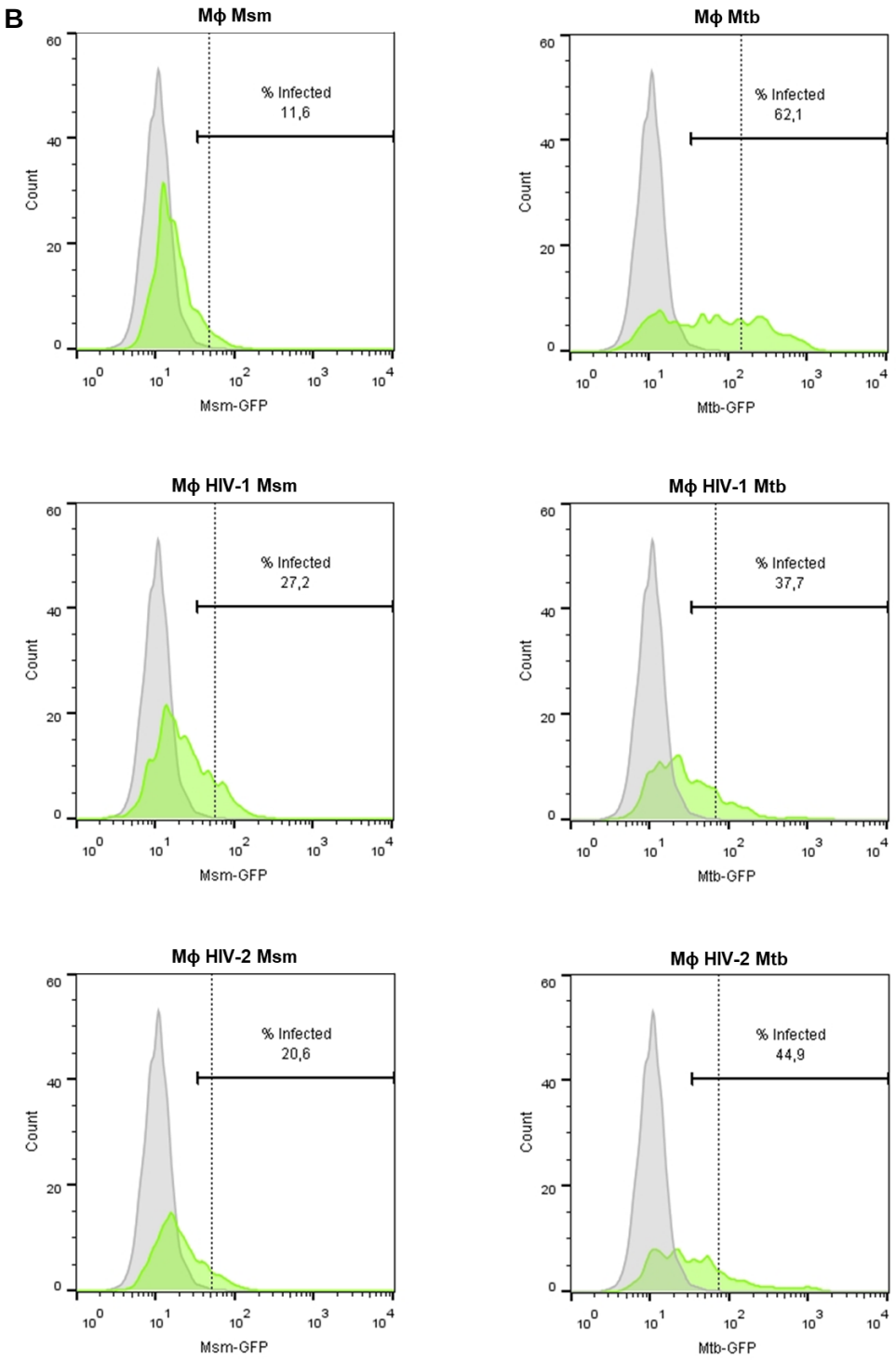

Figure 2: Percentage of mycobacteria infected dendritic cells (A) and macrophages (B). Cells were mono-infected with Msm-GFP or Mtb-GFP or co-infected with HIV. Mycobacteria burden was determined 48 h after bacterial infection by flow cytometry and results were analysed using FlowJo®, LCC. Graphs depict the most representative sample for each condition. Non-infected control cells are shown in grey while cells cultivated with the pathogens are shown in green. The gate represents the infected cells and above it is depicted the average percentage of infection (n = 3). The dashed line marks the mean fluorescence intensity for subpopulation of infected cells.

Apoptosis was measured to infer the impact of the experimental procedures on the cells and to determine the effect of each infection in cell viability at the time of cathepsin and cystatin gene expression measurement. DC and Mϕ were mono- and co-infected as before and stained for annexin V and with 7-AAD 48 h after bacterial infection. Annexin V is expressed at the surface of apoptotic cells while 7-AAD binds to the DNA of late apoptotic cells and necrotic cells. The percentage of apoptotic and necrotic cells was measured by flow cytometry.

From the results it can be observed that DC are mainly in an early apoptotic state, with necrotic cells accounting for less than 1 % of the total cell population. HIV infection increases the percentage of late apoptotic cells and reduces the percentage of early apoptotic cells comparatively to bacterial infections (Annex Figure 2).

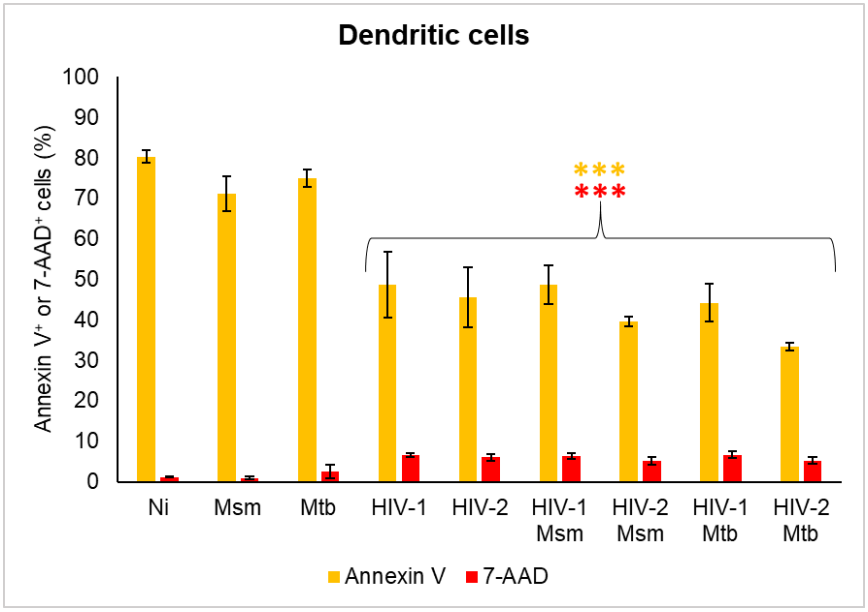

Figure 3: Cell death of dendritic cells mono-infected and co-infected with mycobacteria and virus. DC were infected with HIV-1/HIV-2 and/or Msm/Mtb and stained for annexin V and 7-AAD 48 h after mycobacteria infection. Results were obtained by flow cytometry and are the average of biologic triplicates for each condition. Annexin V and 7-AAD results are shown in yellow and red bars, respectively, being the significance relative to non-infected cells (Ni) (****p* <0.001).

In all infections the percentage of annexin V^+ cells is lower while the percentage of 7-AAD^+ cells is higher than the displayed by non-infected cells (****p*<0.001), except in mycobacteria mono-infections which display no differences (Figure 3). Apart from

Msm and Mtb mono-infections, the remaining infections have a lower percentage of early apoptotic cells and a higher percentage of late apoptotic cells than Ni cells (Annex Figure 2).

Both HIV mono-infections display the same percentage of annexin V and 7-AAD positive cells, leading to the same level of apoptosis and necrosis. In contrast, no differences in apoptosis are shown between mycobacterium mono-infection. However, Mtb mono-infection of DC has a higher percentage of 7-AAD$^+$ cells (*p<0.05) and so has more cells in a late apoptotic or necrotic state.

Between these two classes of pathogens, *Mycobacterium spp* mono-infections display a higher level of annexin V$^+$ cells, mainly caused by higher percentage of early apoptotic cells, while viral mono-infections have a higher level of 7-AAD$^+$ cells (***p<0.001), due to increased levels of late apoptotic cells (Figure 3 and Annex Figure 2).

Among DC infections, Mtb mono-infection has the lowest percentage of live cells. Non-infected cells have the highest level of annexin V staining and the highest percentage of early apoptotic cells among all conditions (Figure 3 and Annex Figure 1).

No differences in apoptotic and necrotic cells between viral mono-infection and co-infections are observed, except for the percentage of annexin V$^+$ cell in HIV-2 Mtb co-infection (*p<0.05) (Figure 3 and Annex Figure 2). In contrast, co-infection leads to a lower percentage of annexin V$^+$ and a higher percentage of 7-AAD$^+$ cells than mycobacteria mono-infections (***p<0.001). Thus, the level of apoptotic and necrotic cells during co-infections is more similar to HIV mono-infections than mycobacteria mono-infections.

Between co-infections, HIV-1 Mtb co-infection induces higher levels of annexin V$^+$ and 7-AAD$^+$ cells than HIV-2 Mtb co-infection, (*p<0.05) (Figure 3 and Annex Figure 2).

Infected Mϕ are mainly in an early apoptotic state, with necrosis still being detected in less than 1 % of all infected cells. For viral infections it is observed an increase in the percentage of late apoptotic cell and a reduction of live cells comparatively to mycobacterium mono-infections (Annex Figure 3).

For all Mϕ infections, the percentage of annexin V^+ and 7-AAD^+ cells is higher than non-infected cells (***p<0.001), except for Msm and Mtb mono-infections in 7-AAD staining (Figure 4 and Annex Figure 1).

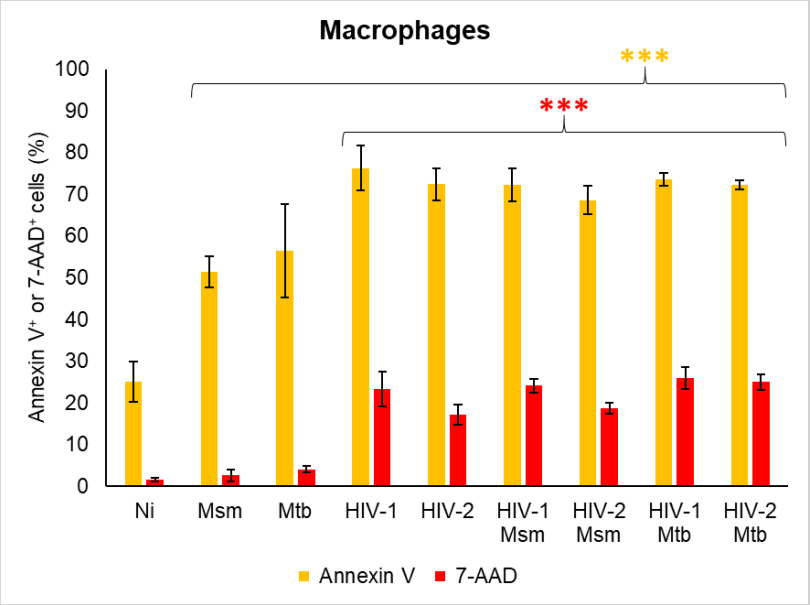

Figure 4: Cell death of macrophages mono-infected or co-infected with mycobacteria and virus. Mϕ were infected with HIV-1/HIV-2 and/or Msm/Mtb and stained for annexin V and 7-AAD 48 h after mycobacteria infection. Results were obtained by flow cytometry and are the average of biologic triplicates for each condition. Annexin V and 7-AAD results are shown in yellow and red bars, respectively, being the significance relative to non-infected cells (Ni) (***p <0.001).

Non-infected cells and Msm mono-infection present the highest percentage of live cells among all conditions and Mϕ infections, respectively (Figure 4 and Annex Figure 3).

Both bacterial species mono-infections lead to the same percentage of apoptotic and necrotic cells while HIV-1 mono-infection of Mϕ leads to a higher percentage 7-AAD^+ cells than HIV-2 (***p=0.001) and no differences in annexin V^+ percentage.

HIV-1 and HIV-2 mono-infections present a higher percentage of annexin V^+ and 7-AAD^+ cells than mycobacterium mono-infections (***p<0.001) (Figure 4 and Annex Figure 3). Thus, viral mono-infections lead to a higher percentage of cell death than mycobacterium mono-infections.

Co-infections have a higher percentage of annexin V^+ and 7-AAD^+ cells (**p<0.01) than mycobacterium mono-infections of Mϕ (Figure 4). In contrast, only HIV-2 Mtb co-infection has a higher level of 7-AAD^+ cells than HIV-2 mono-infection (***p<0.001), while for the remaining co-infection and the annexin V staining there is no difference. As seen for DC, co-infections resemble more closely to HIV infections in terms of cell death.

Among Mϕ co-infections, HIV-2 Msm has a lower percentage of apoptotic and necrotic cells than HIV-2 Mtb co-infections (***p=0.001) and HIV-1 Msm has lower percentage of 7-AAD^+ cells than HIV-2 Msm co-infections (**p<0.01) (Figure 4).

2. Gene expression profile of cathepsins and cystatins in macrophages and dendritic cells

To elucidate the effect of mycobacteria and HIV in the gene expression of cathepsins and cystatins during co-infection it is useful to know how these pathogens regulate these proteins during mono-infection. This was already studied for Msm and Mtb mono-infections in Mϕ but not in DC [84] and for HIV-1 and HIV-2 mono-infections this type of gene expression screen was not yet performed.

Monocyte-derived Mϕ and DC were infected with HIV-1 or HIV-2 (1 ng of reverse transcriptase per 9 x 10^5 cells) for 24 h and with Msm or Mtb (MOI 1) for 3 h. All samples were subjected to the same procedure and cathepsin and cystatin gene expression was measured 48 h after mycobacteria infection (Figure 5).

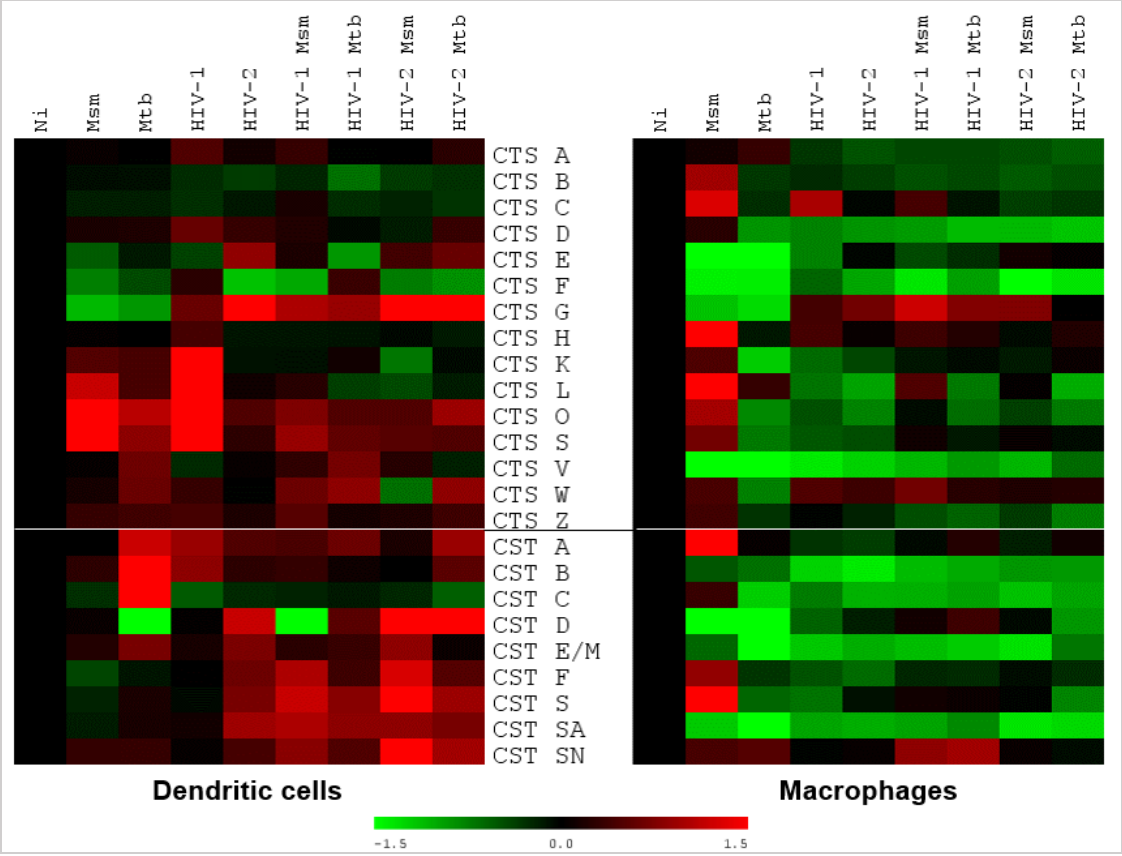

Figure 5: Gene expression of cathepsins (CTS) and cystatins (CST) in dendritic cells and macrophages infected with Msm, Mtb, HIV-1 and/or HIV-2. mRNA levels were quantified by real-time reverse transcriptase PCR 48 h after mycobacterium infection. Values of gene expression are depicted in a heatmap (MeV, MultiExpreriment Viewer) and represented as $\log_2$ relatively to non-infected cells (Ni).

a. *Infections of dendritic cells lead to a general upregulation profile relatively to macrophages.*

Both mycobacteria and HIV mono- and co-infections of DC display an upregulation profile when comparing with the infection of Mϕ (red relatively to green on Figure 5). For Mϕ, Msm infection leads to an upregulation profile, as expected from a species that is efficiently cleared by Mϕ. Mtb infection of Mϕ leads to a downregulation profile with only cathepsin A, L, cystatin A and SN being overexpressed.

Msm and Mtb mono-infection lead to a differential expression of cystatin A, C, D, S and SA genes in DC, being all downregulated during Msm mono-infection except cystatin D gene. It is expectable that an upregulation of cathepsins during Msm infection will be accompanied by a downregulation of their inhibitors for enzymatic activity and bacteria killing. In Mϕ this is observed for cathepsin B, C, D, H, K, L, O, S, W and Z, being all upregulated during Msm mono-infection.

The least expressed genes during Msm infection are cathepsin G gene for DC and cathepsin E, F, V and cystatin D genes for Mϕ. During Mtb infection, in DC it is observed that cathepsin G and cystatin D genes are strongly downregulated, while in Mϕ this is seen for cathepsin E, V, cystatin D, E/M and SA genes.

In contrast, the most overexpressed genes during Msm infection are cathepsin L, O and S genes in DC and cathepsin H, L and cystatin S in Mϕ. For Mtb mono-infection this is seen for cystatin B and C in DC and cystatin SN in Mϕ.

During co-infections, DC are overexpressing the analysed genes, particularly cystatin genes, whereas Mϕ are downregulating them (Figure 5). These profiles are accompanied by higher levels of upregulation and lower levels of downregulation during DC co-infections comparatively to Mϕ and the inverse is seen in Mϕ co-infections in comparison with DC.

Although in different levels, all the co-infections studied have cathepsin G as one of most upregulated genes during DC and Mϕ co-infection, except for HIV-2 Mtb co-infection of Mϕ, and cathepsin F as one of most downregulated genes, apart from of HIV-1 Mtb co-infection of DC.

When comparing Msm with Mtb co-infections, the non-pathogenic mycobacteria co-infections have higher levels of gene upregulation in DC and Mϕ than pathogenic

mycobacteria co-infections. During Mtb co-infections, DC show a differential expression of cathepsin A, D, E, F, K and V genes, while in Mϕ this is seen for cathepsin E, K, cystatin D, S and SN genes.

b. *HIV mono-infections lead to an opposite expression profile of cathepsin and cystatin genes between dendritic cells and macrophages.*

During HIV-1 and HIV-2 mono-infections, the expression of cathepsin and cystatin genes is upregulated in DC and downregulated in Mϕ (Figure 5). The exceptions to this general profile in DC are cathepsin B, C and cystatin C genes, which are repressed, and in Mϕ are cathepsin G, H and W genes, which are overexpressed.

The results obtained show that HIV-1 and HIV-2 mono-infections lead to a differential expression of cathepsin E, F, H, K, V, W and cystatin S genes in DC and of cathepsin C in Mϕ.

Cathepsin K, L, O and S genes in HIV-1 infected DC and cathepsin G and cystatin D genes in HIV-2 infected DC are the most upregulated genes. In opposition, cathepsin E and cystatin C genes in HIV-1 infected DC and cathepsin F in HIV-2 infected DC are the most downregulated genes.

In Mϕ, cathepsin C and cathepsin G genes are the most upregulated during HIV-1 and HIV-2 infections, respectively. The least expressed genes are cathepsin V, cystatin B and E/M genes in both HIV infections of Mϕ.

c. *Comparison of Mtb and HIV-1 mono-infections with HIV-1 Mtb co-infection*

When comparing HIV-1 and Mtb mono-infections (Figure 6), cathepsin A, F, G, V, cystatin C, D, F and S genes in DC and cathepsin A, C, G, H, L, W, cystatin A and SN genes in Mϕ are differentially expressed between mono-infections. During co-infection, the expression profile of these genes is, for the majority, the same as the observed for HIV-1 mono-infection.

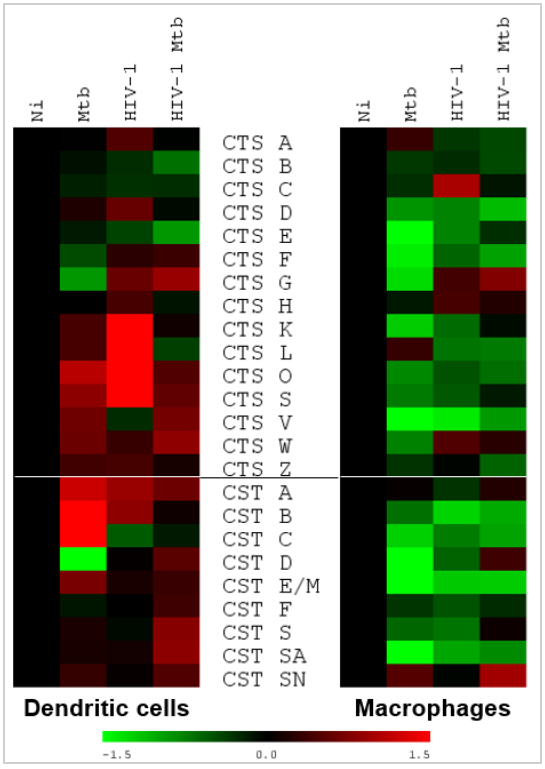

Figure 6: Gene expression of dendritic cells and macrophages mono-infected with HIV-1 or Mtb and co-infected with both pathogens. mRNA levels were quantified by real-time reverse transcriptase PCR 48 h after mycobacterium infection. Values of gene expression are depicted in a heatmap (MeV, MultiExpreriment Viewer) and represented as $\log_2$ relatively to non-infected cells (Ni).

During HIV-1 Mtb co-infection, DC have an upregulation profile, except for cathepsin A, B, C, D, E, H, L and cystatin C genes, whereas Mϕ display a downregulation profile except for cathepsin G, H, W, cystatin A, D and SN genes. From these, cathepsin D, H and L genes (DC) display a shift from upregulated during mono-infection to downregulated during co-infection and cystatin D (Mϕ) displays the opposite shift.

While cathepsin B and E (DC), cathepsin B, D and Z genes (Mϕ) have a stronger downregulation, cathepsin W and cystatin SA (DC) have a stronger overexpression during HIV-1 Mtb co-infection comparatively to both mono-infections, suggesting that both pathogens have a cumulative effect.

During co-infection, cathepsin A and L (Mϕ) are more repressed and cathepsin F, G, cystatin D, F and S genes (DC) are more expressed than in HIV-1 infection. In opposition, for Mϕ cathepsin E, K, S, V, cystatin F and SA genes are less repressed in HIV-1 Mtb co-infection than in both mono-infections and cathepsin G, cystatin A and SN than one of the mono-infections.

d. *Comparison of Mtb and HIV-2 mono-infection with HIV-2 Mtb co-infection*

When comparing HIV-2 and Mtb mono-infections (Figure 7), it is observed a differential expression of cathepsin A, G, H, L, W and cystatin A genes in Mϕ and of cathepsin A, E, G, H, K, W, cystatin C, D and F genes in DC. As in HIV-1 Mtb co-infection, most of these genes display the same expression profile as HIV-2 mono-infection.

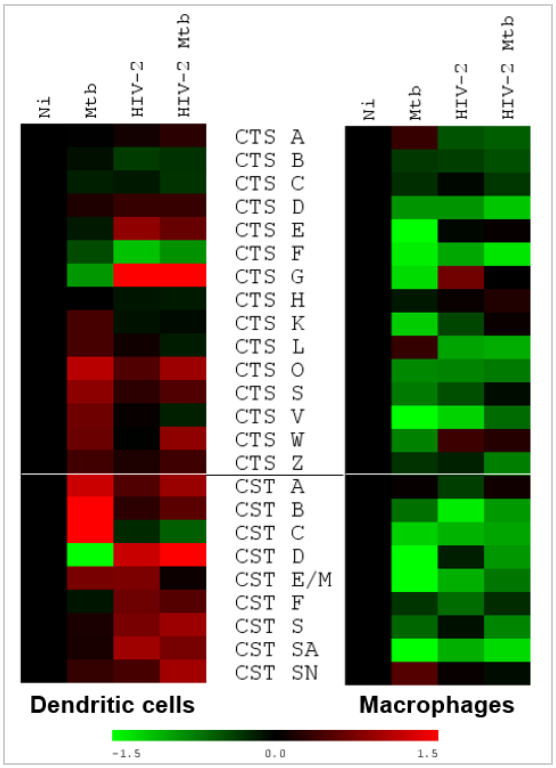

Figure 7: Gene expression of dendritic cells and macrophages mono-infected with HIV-2 or Mtb and co-infected with both pathogens. mRNA levels were quantified by real-time reverse transcriptase PCR 48 h after mycobacterium infection. Values of gene expression are depicted in a heatmap (MeV, MultiExpreriment Viewer) and represented as $\log_2$ relatively to non-infected cells (Ni).

DC co-infected with HIV-2 and Mtb display an upregulation profile, except for cathepsin B, C, F, H, K, L, V and cystatin C genes. In contrast, co-infected Mϕ have a downregulation profile, apart from cathepsin E, G, H, K, W and cystatin A genes.

This co-infection increases the upregulation level of cathepsin A, D, W, cystatin S, SN (DC), cathepsin H and cystatin A (Mϕ) genes and leads to a stronger repression of cathepsin C, H, (DC), B, C, D, Z and cystatin S (Mϕ) comparatively to HIV-2 and Mtb mono-infections. Cathepsin L, V, cystatin C (DC), cathepsin A and L (Mϕ) expression is

further repressed in co-infection comparatively to HIV-2 mono-infection, and cathepsin O, S, V, cystatin C, E/M and F (Mϕ) genes are less downregulated in co-infection.

Cathepsin E, K and cystatin SN (Mϕ) shift from downregulated during mono-infections to upregulated during this co-infection and cathepsin L and V (DC) genes display the opposite shift.

3. Control of cathepsin S expression by *Mycobacterium tuberculosis*

Among cathepsins, cathepsin S participates in phagocytosis, endocytosis, autophagy, apoptosis and antigen processing and presentation and it is mainly expressed in antigen presenting cells. In the present study it is shown that the expression of cathepsin S is downregulated during Mtb, HIV-1 and HIV-2 mono and co-infections of Mϕ comparatively to Msm mono-infection. This suggests that these pathogens are manipulating the gene expression of this protein. In order to elucidate how these pathogens manipulate cathepsin S expression and to further gain control of this protease during infection, in a first approach it was evaluated the contribution of miRNAs during Mtb infection of Mϕ.

a. *miR-106b-5p expression is induced by Mtb and cathepsin S expression is modulated by miR-106b-5p*

A global transcriptomic analysis in the J774A.1 cells, a murine Mϕ cell line, previously showed that there are 36 miRNAs that are modulated during Msm infection, being miR-32, miR-106b-5p, miR-142-3p and miR-142-5p the most differentially regulated [79]. Thus, Mtb may manipulate these miRNAs relatively to Msm, revealing an additional pathogenic mechanism. To access this possible manipulation, the expression of these miRNAs in human Mϕ infected with Mtb was measured 1, 4 and 24 h postinfection.

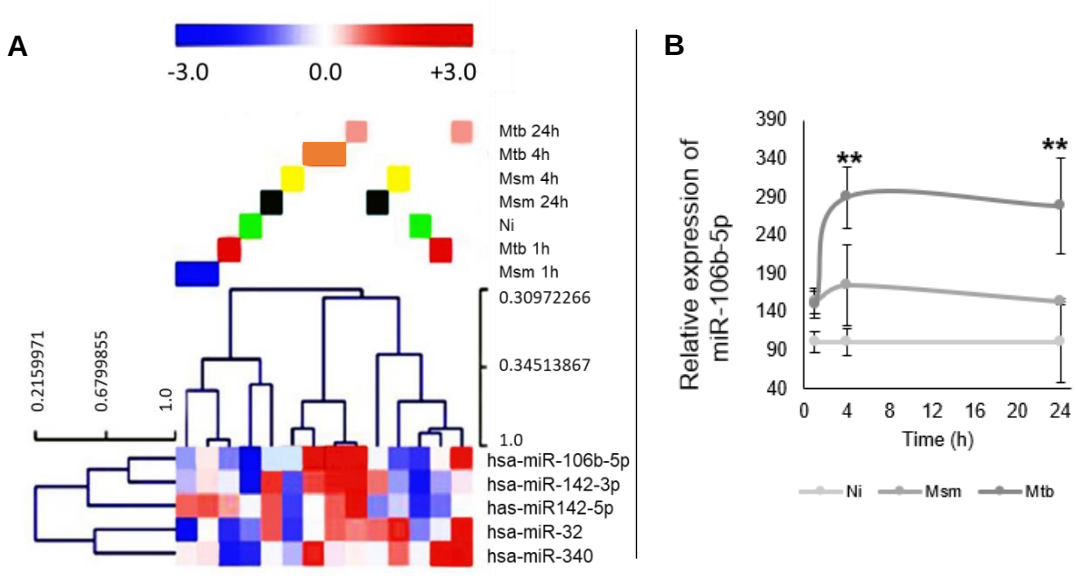

Figure 8: miR-106b-5p expression is upregulated during Mtb mono-infection of macrophages. RNA from non-infected, Msm and Mtb infected Mϕ was extracted and quantified by real-time reverse transcriptase PCR at 1, 4 and 24 h postinfection. (A) Relative quantification of miRNA expression depicted as a heat map with hierarchical clustering performed by Exiqon. Each row represents a miRNA and each column a sample. Sample colour: pink - Mtb 24 h; orange - Mtb 4 h; yellow - Msm 4 h; black - Msm 24 h; green - non-infected cells (Ni) red - Mtb 1 h; blue - Msm 1 h. Colour scale: red – expression above the mean, blue - expression bellow the mean. (B) Specific quantification of miR-106b-5p expression. Values are relative to Ni and are the average of biological triplicates. Error bars show the standard error and the respective significance between samples is shown above (**p <0.01).

Among the studied miRNAs, miR-106b-5p is highly expressed during Mtb infection of Mϕ (4 h and 24 h) comparatively to non-infected and Msm mono-infected Mϕ (Figure 8 A). The expression of miR-106b-5p in Mϕ increases 2-folds after 4 h and 24 h of Mtb mono-infection in comparison with non-infected cells, whereas Msm infection doesn't alter the expression of this miRNA (Figure 8 B).

Due to the high expression levels of miR-106b-5p during Mtb infection of Mϕ, to cathepsin S being a predicted targeted of miR-106b-5p (miRanda, miRtaget2 and miRmap tools [85–87]) and since it has binding sites for this miRNA [88], it was measured the effect of this miRNA on the protein expression of cathepsin S. Non-infected Mϕ were transfected with a non-targeting miRNA (control), a miR-106b-5p mimic and a miR-106b-5p inhibitor and after protein extraction, protein levels were determined by western blot (Figure 9).

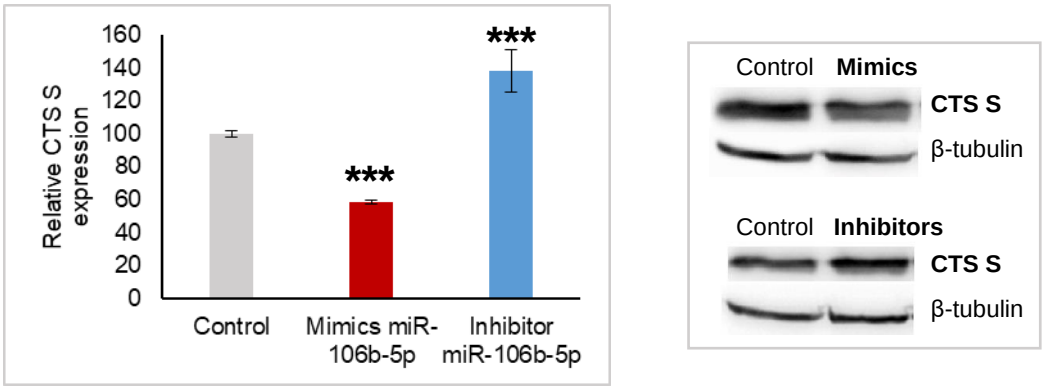

Figure 9: Cathepsin S expression is modulated by miR-106b-5p in non-infected macrophages. Cathepsin S protein levels of non-infected Mϕ was determined by western blot after transfection with miR-106b-5p mimics and inhibitors. CTS S expression is relative to non-targeting miRNA (control) and was determined by measuring the intensity of the western blot bands using ImageJ. The depict values are the average of biological duplicates and the respective significance is relative to the control (***p<0.001).

When Mϕ were transfected with miR-106b-5p mimic and so induced to overexpress this molecule, the expression of cathepsin S decreased almost 4-folds, whereas when transfected with miR-106b-5p inhibitors and thus repressing the action of this molecule, the expression decreased almost 4-folds comparatively to the control (Figure 9).

b. *miR-106b-5p reduces cathepsin S protein expression during Mtb infection of macrophages*

Cathepsin S expression is downregulated during Mtb infection of Mϕ (Figure 5) and transfection of non-infected Mϕ with miR-106b-5p mimic lowers the protein levels of this protein (Figure 9). To determine if this repression is caused by the action of miR-106b-5p during Mtb infection, Mϕ were transfected with a non-targeting miRNA (control), a miR-106b-5p mimic and a miR-106b-5p inhibitor, infected with Mtb and protein expression was determined by western blot (Figure 10).

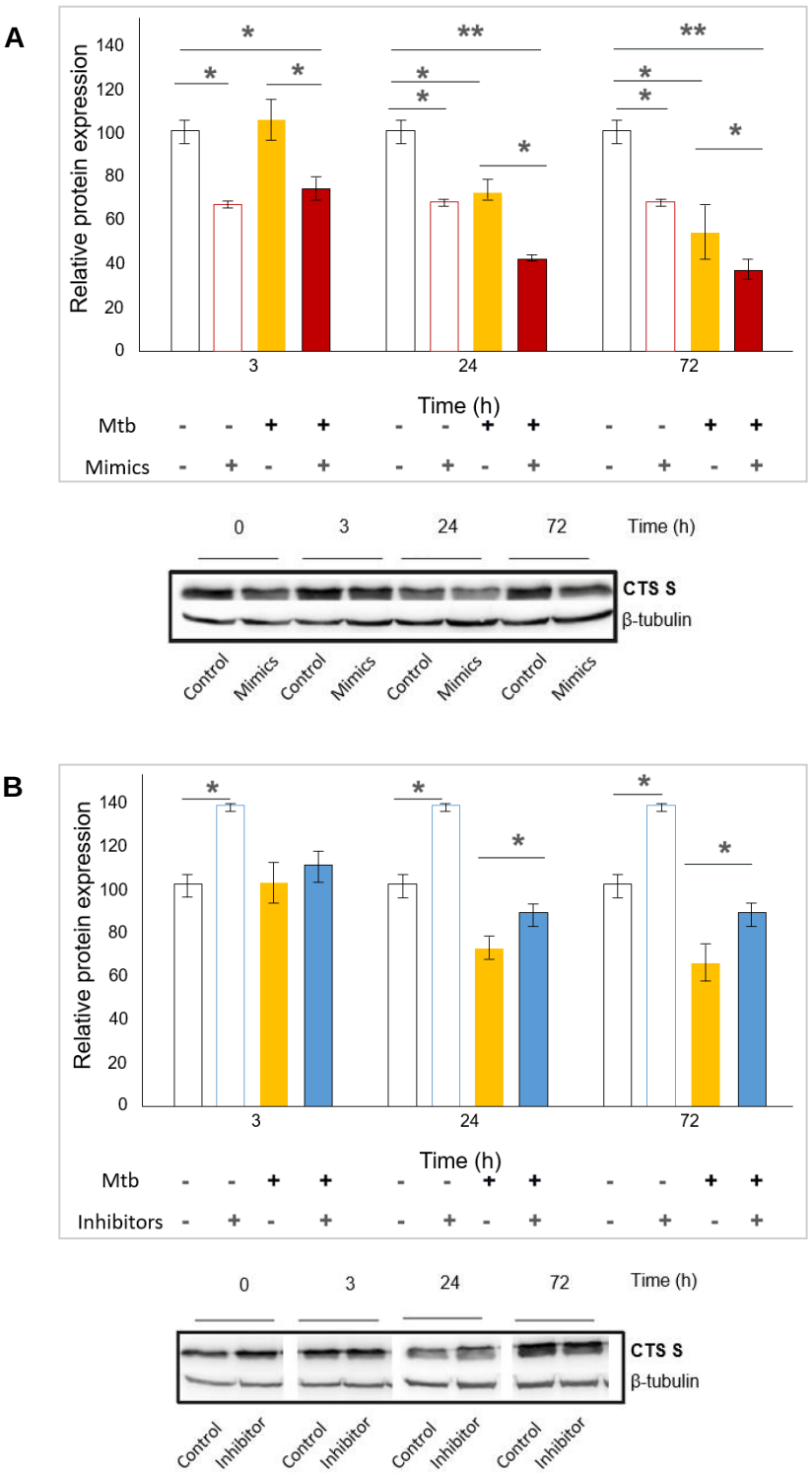

Figure 10: Cathepsin S expression is modulated by miR-106b-5p during Mtb infection of macrophages. Cathepsin S protein levels of Mϕ transfected with (A) miR-106b-5p mimics and (B) miR-106b-5p inhibitors was determine by western blot after transfection with miR-106b-5p mimcs and inhibitors. CTS S expression is relative to non-targeting miRNA (control) and was determined by measuring the intensity of the western blot bands using ImageJ. The depict values are the average of biological duplicates and the respective significance is relative to the control (***p<0.001).

Mtb mono-infection of Mϕ decreases the protein level of cathepsin S when these cells are transfected with miR-106b-5p mimics as early as 3 h postinfection comparatively to Mϕ transfected with non-targeting miRNA (Figure 10 A). For Mϕ transfected with miR-106b-5p inhibitors and mono-infected with Mtb, the protein expression of cathepsin S significantly increases 24 h and 72 h postinfection (Figure 10 B).

During later stages of infections (24 h and 72 h), Mtb reduces the protein levels of cathepsin S comparatively to non-infected Mϕ (Figure 10, yellow bar vs. black limited bar). Infected Mϕ transfected with miR-106b-5p mimics display a stronger repression at 3, 24 and 72 h postinfection, whereas cells transfected with miR-106b-5p inhibitors have an increase of cathepsin S protein expression at 24 h and 72 h postinfection comparatively to Mtb mono-infected Mϕ (*$p<0.05$).

Thus, Mtb infection reduces the protein expression of cathepsin S and miR-106b-5p modulates this protease expression during Mtb infection of Mϕ.

c. *miR-106b-5p increases Mtb intracellular survival in Mϕ*

Cathepsin S participates in cell death through apoptosis, necrosis, autophagy contributing to the control of infections [89]. Since miR-106b-5p modulates the expression of cathepsin S during Mtb infection, it was determined the role of miR-106b-5p in the intracellular survival of Mtb in Mϕ.

Mϕ were transfected with a small interfering RNA (siRNA) against cathepsin S, to confirm that the action of this protein alters Mtb survival, since these RNA molecules degrade the target mRNA, with miR-106b-5p mimics and inhibitors to overexpress or repress this miRNA.

When miR-106b-5p is being overexpressed Mtb survival increases comparatively to control Mϕ, particularly after 3 and 5 days postinfection (Figure 11, red line). This decrease in Mtb killing is also seen when transfecting Mϕ with cathepsin S siRNA (orange line). In contrast, Mtb infected Mϕ transfected with miR-106b-5p inhibitor have a decrease in mycobacterium survival 3 and 5 days after infection (Figure 11, blue line).

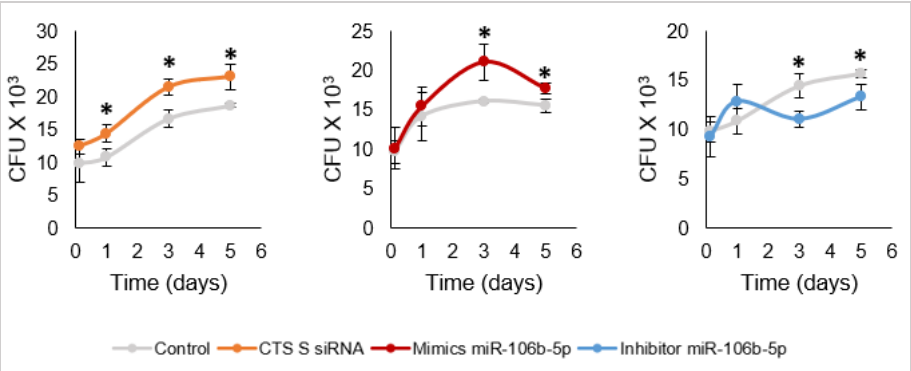

Figure 11: miR-106b-5p modulates Mtb survival in macrophages. Cells transfected with miR-106b-5p mimics or inhibitors were infected with Mtb and lysed after 3 h, 1, 3 and 5 days postinfection. Intracellular mycobacteria was quantified by colony forming units and the depict values are the average of biological triplicates measured in duplicates. The standard error and the statistically significance comparatively to the control are shown for each time-point (*p<0.05).

Given that Mtb killing decreases when Mϕ are overexpressing miR-106b-5p, it was determined the involvement of apoptosis, necrosis and autophagy in Mtb survival 24 h postinfection.

As seen in Figure 12, when Mtb infected Mϕ are overexpressing or repressing miR-106b-5p the percentage of apoptotic and necrotic cells is maintained comparatively to control miRNA, with this also occurring when cathepsin S mRNA is degraded.

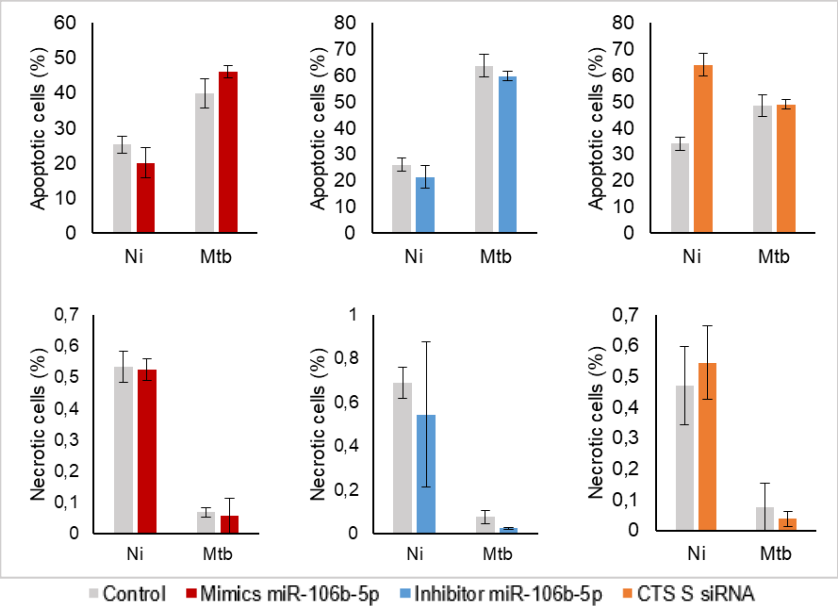

Figure 12: miR-106b-5p effect on Mtb survival in macrophages is independent from apoptosis and necrosis. Percentage of apoptotic and necrotic Mtb infected Mϕ was measured by flow cytometry after staining transfected cells 24 h postinfection with annexin V and propidium iodide. It is shown one representative experiment performed in triplicate.

As for autophagy, in Mtb infected Mϕ staining of LC3, a cytosolic protein which upon autophagy is recruited to autophagosome membranes [90], revealed that neither miR-106b-5p mimics nor inhibitors modulate this pathway, although Mtb infection of non-transfected Mϕ increased LC3 staining (Figure 13).

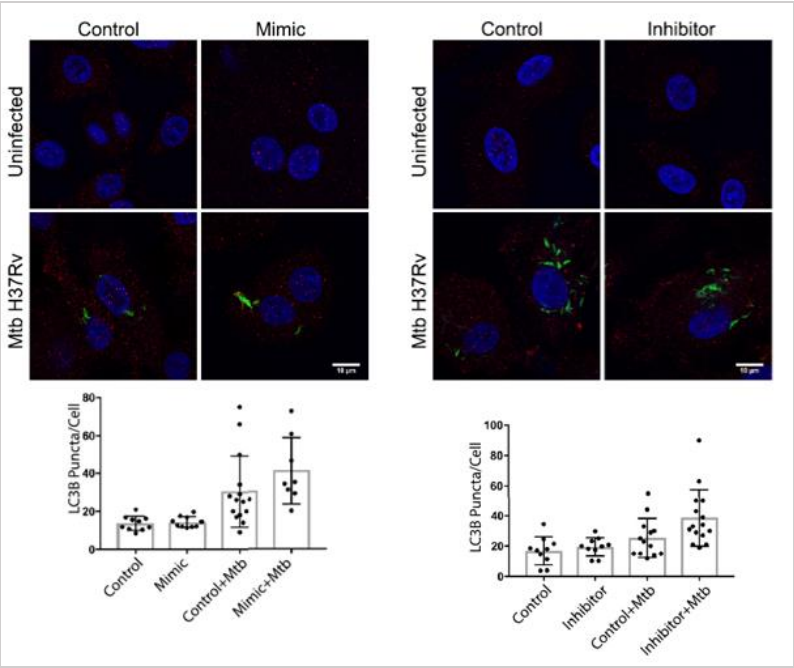

Figure 13: miR-106b-5p effect on Mtb survival in macrophages is independent from autophagy. LC3 and cell nuclei were stained 24 h after Mtb-GFP infection of transfected Mϕ. Results were visualized by confocal microscopy and quantified with ImageJ. LC3, nuclei and Mtb are stained in red, blue and green, respectively. Each bar plot represents the mean of 8 microscopy fields from one representative experiment.

Although the intracellular survival of Mtb increases due to miR-106b-5p action and when cathepsin S is knocked-down, neither apoptosis, necrosis nor autophagy are involved.

d. *miR-106b-5p modulates antigen presentation machinery and T-cell priming*

Cathepsin S is known to participate in antigen presentation by degrading the invariant chain of the MHC class II molecules [91–93]. Since miR-106b-5p reduces the protein levels of this protease during Mtb infection, the effect of this molecule on antigen presentation was determined through the surface expression of HLA-DR class II molecules.

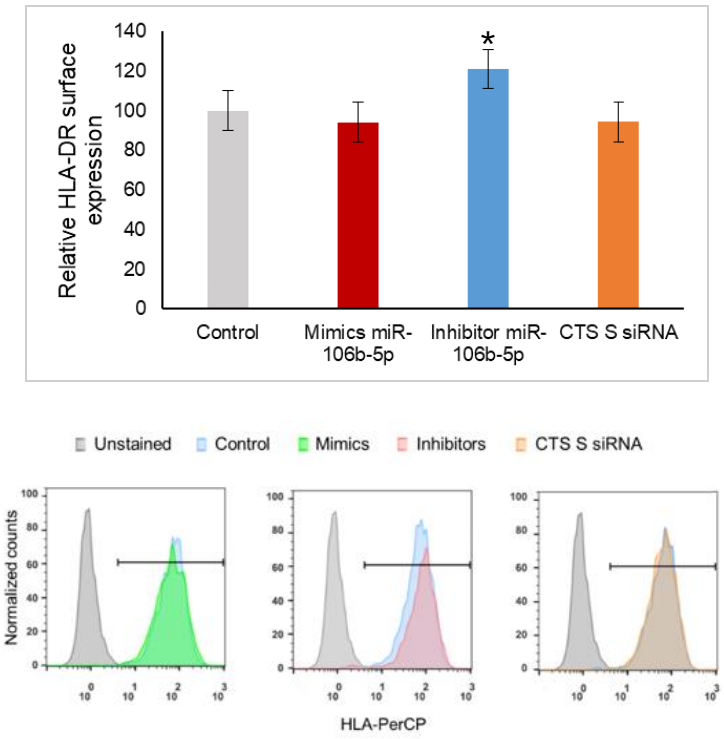

Figure 14: Inhibition of miR-106b-5p increases HLA-DR surface expression in Mtb infected macrophages. HLA-DR surface expression was measured by flow cytometry 24 h after Mtb infection of Mϕ previously transfected with miR-106b-5p mimcs or inhibitor. Bar plots depict the median fluorescence intensity relative to the respective control of one representative experiment performed in triplicates. The statistical significance is shown above the error bar (*p<0.05).

While neither miR-106b-5p mimics nor CTS S siRNA alter the surface expression of HLA-DR in Mtb mono-infected Mϕ, inhibition of miR-106b-5p leads to an increase in the surface expression of HLA-DR class II molecules (Figure 14).

Since antigen presentation allows T cell priming and activation of the adaptive immune response, T cell proliferation was evaluated by co-culturing Mtb infected Mϕ transfected with control, mimics, inhibitor or siRNA with CD4 T cells for 5 days and quantified by flow cytometry.

As depict in Figure 15, there is an increase in the proliferation of CD4 T cells when the action of miR-106b-5p is inhibited, while for the remaining conditions there is no alteration of T cell proliferation comparatively to the control.

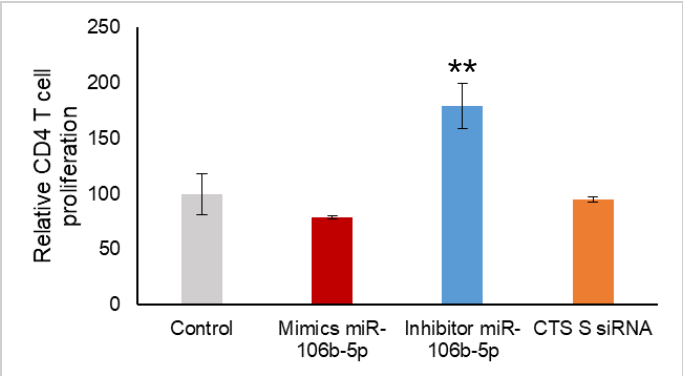

Figure 15: Inhibition of miR-106b-5p increases CD4 T cell proliferation. T cells were cocultured for 5 days with Mtb infected and transfected Mϕ. T cell proliferation was measured by flow cytometry. Bar plot values depict the increase of CD4 T cells relatively to non-infected control samples (**p<0.01).

Thus, miR-106b-5p interferes with antigen presentation during Mtb infection of Mϕ by reducing the expression of HLA-DR class II molecules and consequently impairing CD4 T cell proliferation.

Discussion

In the first part of this thesis it was analysed the gene expression of cathepsins and cystatins during co-infection of HIV-1 and HIV-2 with Mtb in DC and Mϕ. This gene expression was also determined during Msm, Mtb, HIV-1 and HIV-2 mono-infection and during HIV Msm co-infections. In all co-infection experiments, cells were firstly infected with HIV for 24 h followed by 3 h mycobacteria infection. Gene expression was analysed 48 h after mycobacterium infection.

Before the measurement of gene expression, it was determined the viral integration, viral replication and bacterial burden in mono- and co-infections. In the established infection conditions, HIV-1 and HIV-2 integration was detected in both DC and Mϕ revealing that the virus infected the cells and that reverse transcription and provirus integration occurred. By measuring the activity of the reverse transcriptase enzyme, it was confirmed that the HIV clinical isolates used were non-replicative in DC and Mϕ during mono-infection and that Mtb wouldn't alter its replication during co-infection. Mycobacteria burden was also determined and revealed that at the time of gene expression measurement Msm burden was lower than Mtb and that Mϕ had a higher burden than DC in all the infections studied (Figure 2). Msm clearance was expected since this non-pathogenic mycobacterium is efficiently eliminated in these cells [94–96] within 48 h as demonstrated for THP-1, J774 (a mouse macrophage cell line) and human MDMs [97,98]. In Mϕ, the higher percentage of Mtb-GFP positive cells could be due to their increased phagocytic ability comparatively to DC, which was demonstrated to occur in immature and mature monocyte-derived DC upon infection [99] and after infection with Mtb, or due to the capacity of DC to inhibit the growth of Mtb, as seen in mice bone marrow DC and Mϕ [100]. During HIV Mtb co-infection it was observed a decrease of the bacterial burden. This may be explained by prior HIV infection of DC and Mϕ that was shown to impair phagocytosis through actin remodelling defects, downregulation of surface receptors by viral proteins, such as Nef and Tat, among others [101–103].

To infer the impact of infection in cells, particularly in co-infection, apoptosis and necrosis were measured by staining annexin V and 7-AAD. In all infection conditions, cells were mainly apoptotic, with necrosis being detected in less than 1 % of the cells (Annex Figure 2, Annex Figure 3). Mtb modulates cell death in order to survive and in contrast to what was seen, necrosis is usually preferred over apoptosis during infection with virulent mycobacteria [57,104,105].

Mϕ show a higher percentage of annexin V and 7-AAD positive cells than DC during HIV mono-infections and all co-infections, with DC in an early apoptotic state and Mϕ both in early and late apoptotic state. This shift towards a late apoptotic state is accompanied by a decrease in the percentage of live cells for Mϕ comparatively to DC. Thus, Mϕ may be more efficient in inducing apoptosis than DC upon non-replicative viral infection.

DC mycobacteria mono-infections didn't alter the percentage of annexin V and 7-AAD positive cells comparatively to Ni cells, which is in accordance with a previous study where it was shown that infection of DC with Mtb H37Rv strain leads to non-apoptotic cell death [106]. Mϕ have a significant increase in annexin V staining during Msm and Mtb mono-infection comparatively to Ni cells. Thus, upon infection cells induce apoptosis, which is a recognized defence mechanism of Mϕ [57].

After characterizing the *in vitro* outcome of mono- and co-infections of HIV and mycobacteria in DCs and Mø, gene expression of cathepsins and cystatins was determined. DC displayed an upregulation profile and Mϕ a downregulation profile of cathepsin and cystatin expression upon mono-infection or co-infection with Msm, Mtb, HIV-1 and HIV-2 (Figure 5).

Both Mtb and Msm mono-infections of DC led to an upregulation profile and all the differentially expressed genes were cystatins – A, C, D, S and SA. Interestingly, Mtb infection only downregulated cystatin D expression. Based on BioGrid database, these cystatins, in exception of cystatin S, interact with cathepsins B, H, L, S and V, and were shown to inhibit the action of these proteases (MEROPS). These proteins are involved in antigen presentation, apoptosis and inflammation [68,69,71] and their knock-down increased Mtb intracellular survival [84]. Except for cathepsin B, the remaining genes are overexpressed during Mtb infections although to a lower extent comparatively to Msm mono-infections. This suggests that in DC Mtb is manipulating cathepsins mainly through their regulators and to some extent directly in their gene expression, and possibly impairing antigen presentation and mycobacteria clearance.

In mycobacteria mono-infections of Mϕ, the upregulation profile seen during Msm infection has not seen during Mtb infection, where only 4 out of 24 genes were upregulated and to lower levels, being one of them cathepsin L. Genes that were highly upregulated during Msm mono-infection, such as cathepsin B, C, H and S, were

downregulated during Mtb mono-infection. Thus, Mtb may impair its intracellular destruction by downregulating both cathepsin and cystatin genes in particular the ones that are differently expressed between these mono-infections.

In HIV mono-infections, DC showed an upregulation profile and Mϕ a downregulation profile, that was also seen in co-infections.

In DC, HIV-1 infection led to a strong upregulation of cathepsin K, L, O, S that was not observed in HIV-2 infection. These cathepsins participate in MHC class II maturation, by degrading the invariant chain of these molecules, and in antigen processing [107,108]. Cathepsin L but not cathepsin S expression were shown to be increased 48 h to 96 h after HIV-1 infection in DC. In addition, cystatin C, one of the regulators of cathepsin L and S, was also shown to have decreased expression [109]. Thus, the results obtained in this thesis are in agreement with the previously published, except for cathepsin S.

While DC showed clear differences in gene expression between HIV mono-infections, Mϕ displayed a very similar expression profile with only cathepsin C differentially expressed, being upregulated in HIV-1 infection and weakly downregulated in HIV-2 infection. Differentially expressed genes among viral mono-infections may hinder a specific signature of each HIV. In fact, HIV Mtb co-infections of DC showed the same expression profile of cathepsin E, F and K as in mono-infection.

Co-infection with non-pathogenic mycobacteria leads to higher upregulation levels than with pathogenic mycobacteria, suggesting that although there is prior activation due to HIV-1 and HIV-2 infection, Mtb and not Msm may manipulate gene expression of cathepsins and cystatins.

Among co-infection and in HIV mono-infections, cathepsin G is highly expressed in DC and Mϕ. The downregulation of this protease during mycobacteria mono-infections was also shown to occur in THP-1 and U937 cell lines infected with Mtb *in vitro*. Decreased protein levels and activity of cathepsins G during Mtb infection in these cells were accompanied by an increase in the intracellular survival of this bacteria, which was also seen in monocyte-derived macrophages [84,110,111]. Mice with a knockout in cathepsin G have increased mycobacteria survival and are less able to contain the infection in the lung [112]. These results suggest that Mtb downregulates cathepsin G expression to increase its survival within cells, however Msm, which is eliminated from cells also represses this cathepsin. Cathepsin G was shown to interact with the viral gp120 protein, to interfere and to cleave RANTES, (a chemokine that binds to CCR5 receptor inhibiting HIV-1 entry)[113–117]. Furthermore, this chemokine has

a potent chemotactic activity that enables the recruitmet of cells to the infection site and the inhibition of HIV replication in PBMCs and alveolar Mϕ [118]. Thus, cathepsin G upregulation may be induced by the virus and may impair the cellular response through RANTES.

The most downregulated gene was cathepsin F. This protease cleaves the invariant chain of MHC class II molecules, allowing their maturation [119]. The downregulation of this molecule during DC and Mϕ infections with mycobacteria and HIV may be a way to impair antigen presentation by interfering with MHC class II maturation. Additionally, cathepsin F knock-down was shown to decrease Mtb survival in Mϕ [84], and thus downregulation of protease during infection may be a cellular defence to these pathogens.

When accessing co-infection of DC and Mϕ with HIV-1 or HIV-2 and Mtb, gene expression was controlled by HIV, since differentially regulated genes, such as cathepsin A and cystatin C, display an expression profile similar to HIV. This could have been caused by the order of co-infection, since HIV is the first pathogen to infect the cell. A previous study demonstrated that, with the same order of infection, during co-infection it is Mtb that dominates gene expression, however this study does not analyse cathepsin and cystatin genes [120].

In some cases when mono-infection with HIV and Mtb lead to the same expression profile, during co-infection this appears to be potentiated leading to a further repression or expression of genes, such as cathepsin B in HIV-1 Mtb co-infection and cathepsin C in HIV-2 Mtb co-infection of DC and Mϕ. In contrast, it can also be observed an expression shift from both mono- to co-infection, as seen for cathepsin L which becomes downregulated during HIV-1 and HIV-2 Mtb co-infections of DC and cystatin D which becomes upregulated during HIV-1 Mtb co-infection of Mϕ. This may hinder an additional benefit for both pathogens in the control of the cellular response when in co-infection.

In the second part, it was inferred the involvement of miRNAs in the Mtb manipulation of cathepsin S. These RNA sequences were shown to be relevant not only during Mtb infection but also during other bacterial infections, such as *Pseudomonas aeruginosa* and *Listeria monocytogenes* [78]. Besides the decreased levels of expression of cathepsin S during Mtb mono and HIV Mtb co-infections of Mϕ, in previous studies it was demonstrated that the protein levels of this cathepsins and its activity were decreased comparatively to non-infected cells and Msm infected

cells[84].Thus, it was determined if miRNAs were involved in the decrease of cathepsin S protein expression and the possible consequences of this interaction [75,121].

Firstly, and since several miRNAs had been already demonstrated to be differentially regulated upon Msm infection [79], measurement of the miRNA levels in Mϕ infected with Msm or Mtb revealed that miR-106b-5p was highly expressed during Mtb comparatively to Msm infection and non-infection. To further evaluate the effect of this miRNA in cathepsin S, the protein levels of this protease were measured after transfection of non-infected cells with a mimic or inhibitor of miR-106b-5p. This experiment revealed that indeed miR-106b-5p targets cathepsin S, since miR-106b-5p inhibitor increased cathepsin S expression while miR-106b-5p mimic decreased this parameter.

With the confirmation that miR-106b-5p alters the protein expression of cathepsin S in non-infected Mϕ, it was determined the effect of this miRNAs during Mtb infection of these cells by again transfecting cells with a mimic or inhibitor of miR-106b-5p. When using miR-106b-5p mimic on Mtb infected Mϕ protein levels of cathepsin S increased while using miR-106b-5p inhibitor there was increase. Thus, Mtb infection increases the expression of this miRNA that in turn decreases cathepsin S protein levels.

Given that miR-106b-5p targets and decreases the protein levels of cathepsin S and the role of this protein, it was evaluated the effect of the manipulation of this miRNA in pathogen degradation. While there was an increase in the intracellular survival of Mtb when using miR-106b-5p mimic but not when using inhibitors, no difference between gain and loss-of-function experiments were measured for apoptosis or necrosis comparatively to control cells. While there are reports that show that necrotic cell death aids bacteria clearance others suggest that it enables pathogen escape and dissemination [122,123].

Additionally, autophagy was as not correlated to Mtb intracellular survival upon miR-106b-5p manipulation. However, it was shown that in several cell lines cathepsin S inhibition would lead to autophagy [124] while silencing would lead to the blockage of autophagy [125]. Furthermore, knock-down of cathepsin S was demonstrated to lead to apoptosis and defects in autophagy [126].

With these results and since cathepsin S participates in several distinct steps of the endocytic pathway, it can be suggested that upon phagocytosis Mtb survival via miR-106b-5p results from the hydrolytic activity of cathepsin S along the phagocytic pathway.

The final stage was the determination of the impact of miR-106b-5p in antigen presentation, that is one of the cellular processes in which cathepsin S is known to be involved [92,93]and that Mtb can impair [127–129]. For this, HLA-DR class II surface expression and T cell proliferation upon contact with infected Mϕ were measured. While the use of mimic or siRNA didn't change the surface expression of HLA-DR class II molecules, the use of miR-106b-5p inhibitor increased this expression. Between Msm and Mtb infection, it was already described a decrease in the expression of MHC class II molecules [130]. For T cell proliferation the same profile was observed, having only the miR-106b-5p inhibitor induced an increase in proliferation.

Thus, through miR-106b-5p and consequently through cathepsin S, Mtb modulates both the immune and the adaptive cellular response prolonging its survival within infected cells.

Conclusion

Host directed therapies are emerging as possible complements to standard treatments and therapies. The knowledge of host-pathogen interaction is crucial for this type of therapies since one of the goals is to modulate host factors that are being manipulated by the pathogen to enhance immune response.

Gene expression upon infection may contain a specific signature of each pathogen that can be transposed to co-infection. Cathepsin and cystatin gene expression during *in vitro* Mtb mono-infection of macrophages was already elucidated by our lab[84]. To date it wasn't made a gene expression screen of these proteases and their regulators during HIV co-infections with Mtb. In HIV-1 mono-infection, only specific cathepsins and cystatins have been studied while for HIV-2 mono-infections the number of studies is still scarce, since it affects a lower percentage of persons than HIV-1[131].

From the results obtained in this study, we may conclude that during HIV and Mtb co-infection the gene expression of cathepsins and cystatins is upregulated in DC and downregulated in Mϕ. In addition, HIV gene manipulation appears to prevail over Mtb manipulation during co-infections. New developments are being made in this area as proven by a clinical trial that aims to study gene expression during tuberculosis and HIV co-infection (NCT01611402).

MicroRNAs can be the next tool for host directed therapies and may hinder a potential candidate biomarker, allowing to distinguish the phase of infection in which each patient is. One example is miR-106b-5p which was shown to be downregulated in Mtb latent individuals and upregulated in infected macrophages with Mtb replication[132].

In this study the modulation of miR-106b-5p, and so of cathepsin S expression, allows to conclude that by inhibiting the action of this microRNA Mϕ are more prone to kill Mtb and to activate T cells, enabling the activation of the adaptive immune response.

References

1. WHO. *Global Tuberculosis Report 2017*. *World Health Organization* (2017).
2. Unaids. *2017 Global HIV Statistics*. (2018).
3. Al-Saeedi, M. & Al-Hajoj, S. Diversity and evolution of drug resistance mechanisms in *Mycobacterium tuberculosis*. *Infect. Drug Resist.* **10,** 333–342 (2017).
4. Tang, M. W. & Shafer, R. W. HIV-1 antiretroviral resistance: scientific principles and clinical applications. *Drugs* **72,** e1-25 (2012).
5. Pai, M. *et al.* Tuberculosis. *Nat. Rev. Dis. Prim.* **2,** 1–23 (2016).
6. Matucci, A., Maggi, E. & Vultaggio, A. Cellular and humoral immune responses during tuberculosis infection: Useful knowledge in the era of biological agents. *J. Rheumatol.* **41,** 17–23 (2014).
7. O'Garra, A. *et al.* The Immune Response in Tuberculosis. *Annual Review of Immunology* **31,** 475-527 (2013).
8. Ramakrishnan, L. Revisiting the role of the granuloma in tuberculosis. *Nat. Rev. Immunol.* **12,** 352–366 (2012).
9. Mihret, A. The role of dendritic cells in *Mycobacterium tuberculosis* infection. *Virulence* **3,** 654–659 (2012).
10. Ulrichs, T. & Kaufmann, S. H. E. New insights into the function of granulomas in human tuberculosis. *J. Pathol.* **208,** 261–269 (2006).
11. Saunders, B. M. & Britton, W. J. Life and death in the granuloma: Immunopathology of tuberculosis. *Immunol. Cell Biol.* **85,** 103–111 (2007).
12. Shaw, G. M. & Hunter, E. HIV transmission. *Cold Spring Harb. Perspect. Med.* **2,** (2012).
13. Bracq, L., Xie, M., Benichou, S. & Bouchet, J. Mechanisms for cell-to-cell transmission of HIV-1. *Front. Immunol.* **9,** 1–14 (2018).
14. Law, K. M., Satija, N., Esposito, A. M. & Chen, B. K. Cell-to-Cell Spread of HIV and Viral Pathogenesis. *Advances in Virus Research* **95,** (Elsevier Inc., 2016).
15. Dutartre, H., Clavière, M., Journo, C. & Mahieux, R. Cell-Free versus Cell-to-Cell Infection by Human Immunodeficiency Virus Type 1 and Human T-Lymphotropic Virus Type 1: Exploring the Link among Viral Source, Viral Trafficking, and Viral Replication. *J. Virol.* **90,** 7607–7617 (2016).
16. Tebit, D. M., Ndembi, N., Weinberg, A. & Quiñones-Mateu, M. E. Mucosal transmission of human immunodeficiency virus. *Curr. HIV Res.* **10,** 3–8 (2012).
17. Yu, M. & Vajdy, M. Mucosal HIV transmission and vaccination strategies through oral compared with vaginal and rectal routes. *Expert Opin. Biol. Ther.* **10,** 1181–1195 (2010).
18. World Health Organization. *WHO case definitions of HIV for surveillance and revised clinical staging and immunological classification of HIV-related disease in adults and children*. (2007).

19. Coffin, J. & Swanstrom, R. HIV pathogenesis: dynamics and genetics of viral populations and infected cells. *Cold Spring Harb. Perspect. Med.* **3,** a012526 (2013).

20. Schwartz, S. A. & Nair, M. P. Current concepts in human immunodeficiency virus infection and AIDS. *Clin. Diagn. Lab. Immunol.* **6,** 295–305 (1999).

21. Bell, L. C. K. & Noursadeghi, M. Pathogenesis of HIV-1 and *Mycobacterium tuberculosis* co-infection. *Nat. Rev. Microbiol.* **16,** 80-90 (2018).

22. Pawlowski, A., Jansson, M., Sköld, M., Rottenberg, M. E. & Källenius, G. Tuberculosis and HIV co-infection. *PLoS Pathog.* **8,** (2012).

23. Geldmacher, C. *et al.* Early Depletion of *Mycobacterium tuberculosis* –Specific T Helper 1 Cell Responses after HIV-1 Infection. *J. Infect. Dis.* **198,** 1590–1598 (2008).

24. Shankar, E. M. *et al.* HIV-*Mycobacterium tuberculosis* co-infection: A 'danger-couple model' of disease pathogenesis. *Pathog. Dis.* **70,** 110–118 (2014).

25. Lawn, S. D., Butera, S. T. & Shinnick, T. M. Tuberculosis unleashed: The impact of human immunodeficiency virus infection on the host granulomatous response to *Mycobacterium tuberculosis*. *Microbes Infect.* **4,** 635–646 (2002).

26. Geldmacher, C. *et al.* Preferential infection and depletion of *Mycobacterium tuberculosis* –specific CD4 T cells after HIV-1 infection. *J. Exp. Med.* **207,** 2869–2881 (2010).

27. Kedzierska, K., Crowe, S. M., Turville, S. & Cunningham, A. L. The influence of cytokines, chemokines and their receptors on HIV-1 replication in monocytes and macrophages. *Rev. Med. Virol.* **13,** 39–56 (2003).

28. Imperiali, F. G. *et al.* Increased *Mycobacterium tuberculosis* growth in HIV-1-infected human macrophages: Role of tumour necrosis factor-(alpha). *Clin Exp Immunol* **123,** 435–442 (2001).

29. Pathak, S., Wentzel-Larsen, T. & Åsjö, B. Effects of in vitro HIV-1 infection on mycobacterial growth in peripheral blood monocyte-derived macrophages. *Infect. Immun.* **78,** 4022–4032 (2010).

30. Day, R. B. *et al.* Alveolar Macrophages from HIV-Infected Subjects are Resistant to *Mycobacterium tuberculosis* In Vitro. *Am. J. Respir. Cell Mol. Biol.* **30,** 403–410 (2004).

31. Herbein, G. & Khan, K. A. Is HIV infection a TNF receptor signalling-driven disease? *Trends Immunol.* **29,** 61–7 (2008).

32. Owen, J., Punt, J., Stranford, S., Jones, P. & Kuby, J. *Kuby Immunology*. (W.H. Freeman, 2013).

33. Rosales, C., Uribe-Querol, E. Phagocytosis: a fundamental process in immunity. *Hindawi.* **2017,** (2017).

34. Fairn, G. D. & Grinstein, S. How nascent phagosomes mature to become phagolysosomes. *Trends Immunol.* **33,** 397–405 (2012).

35. Sturgill-Koszycki, S. *et al.* Lack of acidification in *Mycobacterium* phagosomes produced by exclusion of the vesicular proton-ATPase. *Science.* **263,** 678–681 (1994).

36. Queval, C. J. *et al. Mycobacterium tuberculosis* Controls Phagosomal

Acidification by Targeting CISH-Mediated Signaling. *Cell Rep.* **20,** 3188–3198 (2017).

37. Sun, J. *et al. Mycobacterium bovis* BCG disrupts the interaction of Rab7 with RILP contributing to inhibition of phagosome maturation. *J. Leukoc. Biol.* **82,** 1437–1445 (2007).

38. Sun, J. *et al.* Mycobacterial Nucleoside Diphosphate Kinase Blocks Phagosome Maturation in Murine Raw 264.7 Macrophages. *PLoS One* **5,** e8769 (2010).

39. Flannagan, R. S., Cosío, G. & Grinstein, S. Antimicrobial mechanisms of phagocytes and bacterial evasion strategies. *Nat. Rev. Microbiol.* **7,** 355–366 (2009).

40. Von Both, U. *et al. Mycobacterium tuberculosis* Exploits a Molecular off Switch of the Immune System for Intracellular Survival. *Sci. Rep.* **8,** 1–17 (2018).

41. Uribe-Quero, E. & Rosales, C. Control of phagocytosis by microbial pathogens. *Front. Immunol.* **8,** 1–23 (2017).

42. Meena, L. S. & Rajni, T. Survival mechanisms of pathogenic *Mycobacterium tuberculosis* H37Rv. *FEBS Journal* **277,** 2416–2427 (2010).

43. Debaisieux, S. *et al.* HIV-1 Tat inhibits phagocytosis by preventing the recruitment of Cdc42 to the phagocytic cup. *Nat. Commun.* **6,** 6211 (2015).

44. Kedzierska, K. *et al.* HIV-1 Down-Modulates γ Signaling Chain of FcγR in Human Macrophages: A Possible Mechanism for Inhibition of Phagocytosis. *J. Immunol.* **168,** 2895–2903 (2003).

45. Mazzolini, J. *et al.* Inhibition of phagocytosis in HIV-1-infected macrophages relies on Nef-dependent alteration of focal delivery of recycling compartments. *Blood* **115,** 4226–4236 (2010).

46. Yang, Z. & Klionsky, D. J. An overview of the molecular mechanism of autophagy. *Curr. Top. Microbiol. Immunol.* **335,** 1–32 (2009).

47. Baehrecke, E. H. Autophagy: dual roles in life and death? *Nat. Rev. Mol. Cell Biol.* **6,** 505–10 (2005).

48. Kathania, M., Raje, C. I., Raje, M., Dutta, R. K. & Majumdar, S. Bfl-1/A1 acts as a negative regulator of autophagy in mycobacteria infected macrophages. *Int. J. Biochem. Cell Biol.* **43,** 573–585 (2011).

49. Seto, S., Tsujimura, K. & Koide, Y. Coronin-1a inhibits autophagosome formation around *Mycobacterium tuberculosis*-containing phagosomes and assists mycobacterial survival in macrophages. *Cell. Microbiol.* **14,** 710–727 (2012).

50. Espert, L., Beaumelle, B. & Vergne, I. Autophagy in *Mycobacterium tuberculosis* and HIV infections. *Front. Cell. Infect. Microbiol.* **5,** 1–8 (2015).

51. Harding, C. V & Boom, W. H. Regulation of antigen presentation by *Mycobacterium tuberculosis*: a role for Toll-like receptors. *Nat. Rev. Microbiol.* **8,** 296–307 (2010).

52. Portal-Celhay, C. *et al. Mycobacterium tuberculosis* EsxH inhibits ESCRT-dependent CD4+T-cell activation. *Nat. Microbiol.* **2,** 1–9 (2016).

53. Stumptner-Cuvelette, P. *et al.* HIV-1 Nef impairs MHC class II antigen presentation and surface expression. *Proc. Natl. Acad. Sci. U. S. A.* **98,** 12144–9

(2001).

54. Wonderlich, E. R., Leonard, J. A. & Collins, K. L. HIV immune evasion disruption of antigen presentation by the HIV Nef protein. *Adv. Virus Res.* **80,** 103–27 (2011).

55. Elmore, S. Apoptosis: a review of programmed cell death. *Toxicol. Pathol.* **35,** 495–516 (2007).

56. Lam, A. *et al.* Role of apoptosis and autophagy in tuberculosis. *Am. J. Physiol. - Lung Cell. Mol. Physiol.* **313,** L218–L229 (2017).

57. Behar, S. M. *et al.* Apoptosis is an innate defense function of macrophages against Mycobacterium tuberculosis. *Mucosal Immunol.* **4,** 279–287 (2011).

58. Briken, V. Living on the edge: Inhibition of host Cel Apoptosis by *Mycobacterium tuberculosis*. *Future Microbiol.* **3,** 415–422 (2008).

59. Mogga, S. J., Mustafa, T., Sviland, L. & Nilsen, R. Increased Bcl-2 and reduced Bax expression in infected macrophages in slowly progressive primary murine *Mycobacterium tuberculosis* infection. *Scand. J. Immunol.* **56,** 383–391 (2002).

60. Cummins, N. W. & Badley, A. D. Mechanisms of HIV-associated lymphocyte apoptosis: 2010. *Cell Death Dis.* **1,** e99–e99 (2010).

61. Stary, G. *et al.* Plasmacytoid dendritic cells express TRAIL and induce CD4+ T-cell apoptosis in HIV-1 viremic patients. *Blood* **114,** 3854–63 (2009).

62. Le Douce, V., Herbein, G., Rohr, O. & Schwartz, C. Molecular mechanisms of HIV-1 persistence in the monocyte-macrophage lineage. *Retrovirology* **7,** 32 (2010).

63. Swingler, S., Mann, A. M., Zhou, J., Swingler, C. & Stevenson, M. Apoptotic killing of HIV-1-infected macrophages is subverted by the viral envelope glycoprotein. *PLoS Pathog.* **3,** 1281–90 (2007).

64. Mbita, Z., Hull, R. & Dlamini, Z. Human immunodeficiency virus-1 (HIV-1)-mediated apoptosis: New therapeutic targets. *Viruses* **6,** 3181–3227 (2014).

65. Turk, V. *et al.* Cysteine cathepsins: From structure, function and regulation to new frontiers. *Biochim. Biophys. Acta - Proteins Proteomics* **1824,** 68–88 (2012).

66. Stoka, V., Turk, V. & Turk, B. Lysosomal cathepsins and their regulation in aging and neurodegeneration. *Ageing Research Reviews* **32,** 22–37 (2016).

67. Rossi, A., Deveraux, Q., Turk, B. & Sali, A. Comprehensive search for cysteine cathepsins in the human genome. *Biol. Chem.* **385,** 363–372 (2004).

68. Conus, S. & Simon, H. U. Cathepsins and their involvement in immune responses. *Swiss Med. Wkly.* **140,** 1–8 (2010).

69. Colbert, J. D., Matthews, S. P., Miller, G. & Watts, C. Diverse regulatory roles for lysosomal proteases in the immune response. *Eur. J. Immunol.* **39,** 2955–2965 (2009).

70. Turk, B., Turk, D. & Salvesen, G. S. Regulating cysteine protease activity: essential role of protease inhibitors as guardians and regulators. *Curr. Pharm. Des.* **8,** 1623–1637 (2002).

71. Zavašnik-Bergant, T. & Turk, B. Cysteine cathepsins in the immune response. *Tissue Antigens* **67,** 349–355 (2006).

72. Turk, B. *et al.* Regulation of the activity of lysosomal cysteine proteinases by pH-induced inactivation and/or endogenous protein inhibitors, cystatins. *Biol. Chem. Hoppe. Seyler.* **376,** 225–30 (1995).

73. Kramer, L., Turk, D. & Turk, B. The Future of Cysteine Cathepsins in Disease Management. *Trends Pharmacol. Sci.* **38,** 873–898 (2017).

74. Olson, O. C. & Joyce, J. A. Cysteine cathepsin proteases : regulators of cancer progression and therapeutic response. *Nat. Publ. Gr.* **15,** 712–729 (2015).

75. Sabir, N. *et al.* miRNAs in tuberculosis: New avenues for diagnosis and host-directed therapy. *Front. Microbiol.* **9,** 1–14 (2018).

76. He, L. & Hannon, G. J. MicroRNAs: Small RNAs with a big role in gene regulation. *Nat. Rev. Genet.* **5,** 522–531 (2004).

77. Mehta, A. & Baltimore, D. MicroRNAs as regulatory elements in immune system logic. *Nat. Rev. Immunol.* **16,** 279–294 (2016).

78. Zhou, X., Li, X. & Wu, M. miRNAs reshape immunity and inflammatory responses in bacterial infection. *Signal Transduct. Target. Ther.* **3,** 14 (2018).

79. Bettencourt, P. *et al.* Actin-binding protein regulation by microRNAs as a novel microbial strategy to modulate phagocytosis by host cells: the case of N-Wasp and miR-142-3p. *Front. Cell. Infect. Microbiol.* **3,** 19 (2013).

80. Bettencourt, P., Pires, D. & Anes, E. Immunomodulating microRNAs of mycobacterial infections. *Tuberculosis* **97,** 1–7 (2016).

81. Swaminathan, G., Navas-Martín, S. & Martín-García, J. MicroRNAs and HIV-1 infection: Antiviral activities and beyond. *J. Mol. Biol.* **426,** 1178–1197 (2014).

82. Kaufmann, S. H. E., Dorhoi, A., Hotchkiss, R. S. & Bartenschlager, R. Host-directed therapies for bacterial and viral infections. *Nat. Rev. Drug Discov.* **17,** 35–56 (2018).

83. Azevedo-Pereira, J. M. & Santos-Costa, Q. HIV interaction with human host: HIV-2 As a model of a less virulent infection. *AIDS Rev.* **18,** 44–53 (2016).

84. Pires, D. *et al.* Role of Cathepsins in *Mycobacterium tuberculosis* Survival in Human Macrophages. *Sci. Rep.* **6,** 32247 (2016).

85. Betel, D., Wilson, M., Gabow, A., Marks, D. S. & Sander, C. The microRNA.org resource: targets and expression. *Nucleic Acids Res.* **36,** D149–D153 (2007).

86. Vejnar, C. E. & Zdobnov, E. M. miRmap: Comprehensive prediction of microRNA target repression strength. *Nucleic Acids Res.* **40,** 11673–11683 (2012).

87. Wang, X. miRDB: A microRNA target prediction and functional annotation database with a wiki interface. *RNA* **14,** 1012–1017 (2008).

88. Pires, D. *et al. Mycobacterium tuberculosis* Modulates miR-106b-5p to Control Cathepsin S Expression Resulting in Higher Pathogen Survival and Poor T-Cell Activation. *Front. Immunol.* **8,** 1–13 (2017).

89. Repnik, U., Stoka, V., Turk, V. & Turk, B. Lysosomes and lysosomal cathepsins in cell death. *Biochimica et Biophysica Acta - Proteins and Proteomics* **1824,** 22–33 (2012).

90. Tanida, I., Ueno, T. & Kominami, E. LC3 and Autophagy. *Methods in Molecular*

Biology. **445,** 77–88 (Humana Press, 2008).

91. Riese, R. J. *et al.* Cathepsin S activity regulates antigen presentation and immunity. *J. Clin. Invest.* **101,** 2351–2363 (1998).

92. Costantino, C. M., Ploegh, H. L. & Hafler, D. A. Cathepsin S regulates class II MHC processing in human CD4+ HLA-DR+ T cells. *J. Immunol.* **183,** 945–952 (2009).

93. Driessen, C. *et al.* Cathepsin S Controls the Trafficking and Maturation of MHC Class II Molecules in Dendritic Cells. *JCB.* **147,** 775–790 (1999).

94. Bohsali, A., Abdalla, H., Velmurugan, K. & Briken, V. The non-pathogenic mycobacteria *M. smegmatis* and *M. fortuitum* induce rapid host cell apoptosis via a caspase-3 and TNF dependent pathway. *BMC Microbiol.* **10,** 237 (2010).

95. Kuehnel, M. P. *et al.* Characterization of the intracellular survival of *Mycobacterium avium ssp*. paratuberculosis: Phagosomal pH and fusogenicity in J774 macrophages compared with other mycobacteria. *Cell. Microbiol.* **3,** 551–566 (2001).

96. Denis, M., Forget, A., Pelletier, M., Gervais, F. & Skamene, E. Killing of *Mycobacterium smegmatis* by macrophages from genetically susceptible and resistant mice. *J. Leukoc. Biol.* **47,** 25–30 (1990).

97. Anes, E. *et al.* Dynamic life and death interactions between *mycobacterium smegmatis* and J774 macrophages. *Cell. Microbiol.* **8,** 939–960 (2006).

98. Jordao, L., Bleck, C. K. E., Mayorga, L., Griffiths, G. & Anes, E. On the killing of mycobacteria by macrophages. *Cell. Microbiol.* **10,** 529–548 (2008).

99. Nagl, M. *et al.* Phagocytosis and killing of bacteria by professional phagocytes and dendritic cells. *Clin. Diagn. Lab. Immunol.* **9,** 1165–8 (2002).

100. Bodnar, K. A., Serbina, N. V & Flynn, J. L. Fate of *Mycobacterium tuberculosis* within murine dendritic cells. *Infect. Immun.* **69,** 800–9 (2001).

101. Lê-Bury, G. & Niedergang, F. Defective Phagocytic Properties of HIV-Infected Macrophages: How Might They Be Implicated in the Development of Invasive *Salmonella Typhimurium*? *Front. Immunol.* **9,** 531 (2018).

102. Debaisieux, S. *et al.* HIV-1 Tat inhibits phagocytosis by preventing the recruitment of Cdc42 to the phagocytic cup. *Nat. Commun.* **6,** 6211 (2015).

103. Michailidis, C. *et al.* Impaired phagocytosis among patients infected by the human immunodeficiency virus: Implication for a role of highly active anti-retroviral therapy. *Clin. Exp. Immunol.* **167,** 499–504 (2012).

104. Abebe, M. *et al.* Modulation of cell death by M. tuberculosis as a strategy for pathogen survival. *Clin. Dev. Immunol.* **2011,** 678570 (2011).

105. Behar, S. M., Divangahi, M. & Remold, H. G. Evasion of innate immunity by *mycobacterium tuberculosis*: Is death an exit strategy? *Nat. Rev. Microbiol.* **8,** 668–674 (2010).

106. Ryan, R. C., O'Sullivan, M. P. & Keane, J. *Mycobacterium tuberculosis* infection induces non-apoptotic cell death of human dendritic cells. *BMC Microbiol.* **11,** 237 (2011).

107. Hsieh, C.-S., deRoos, P., Honey, K., Beers, C. & Rudensky, A. Y. A Role for Cathepsin L and Cathepsin S in Peptide Generation for MHC Class II

Presentation. *J. Immunol.* **168,** 2618–2625 (2002).

108. Bania, J. *et al.* Human cathepsin S, but not cathepsin L, degrades efficiently MHC class II-associated invariant chain in nonprofessional APCs. *Proc. Natl. Acad. Sci. U. S. A.* **100,** 6664–9 (2003).

109. Harman, A. N. *et al.* HIV-1-infected dendritic cells show 2 phases of gene expression changes, with lysosomal enzyme activity decreased during the second phase. *Blood* **114,** 85–94 (2009).

110. Rivera-Marrero, C. A., Stewart, J., Shafer, W. M. & Roman, J. The down-regulation of cathepsin G in THP-1 monocytes after infection with *Mycobacterium tuberculosis* is associated with increased intracellular survival of bacilli. *Infect. Immun.* **72,** 5712–21 (2004).

111. Danelishvili, L., Everman, J. L., McNamara, M. J. & Bermudez, L. E. Inhibition of the Plasma-Membrane-Associated Serine Protease Cathepsin G by *Mycobacterium tuberculosis* Rv3364c Suppresses Caspase-1 and Pyroptosis in Macrophages. *Front. Microbiol.* **2,** 281 (2011).

112. Steinwede, K. *et al.* Cathepsin G and Neutrophil Elastase Contribute to Lung-Protective Immunity against Mycobacterial Infections in Mice. *J. Immunol.* **188,** 4476–4487 (2012).

113. Levy, J. A. The Unexpected Pleiotropic Activities of RANTES. *J. Immunol.* **182,** 3945–3946 (2009).

114. Cocchi, F. *et al.* Identification of RANTES, MIP-1 alpha, and MIP-1 beta as the major HIV-suppressive factors produced by CD8+ T cells. *Science* **270,** 1811–5 (1995).

115. Aukrust, P., Müller, F. & Frøland, S. S. Circulating levels of RANTES in human immunodeficiency virus type 1 infection: effect of potent antiretroviral therapy. *J. Infect. Dis.* **177,** 1091–6 (1998).

116. Lim, J. K., Lu, W., Hartley, O. & DeVico, A. L. N-terminal proteolytic processing by cathepsin G converts RANTES/CCL5 and related analogs into a truncated 4-68 variant. *J. Leukoc. Biol.* **80,** 1395–1404 (2006).

117. Avril, L. E., Di Martino-Ferrer, M., Pignede, G., Séman, M. & Gauthier, F. Identification of the U-937 membrane-associated proteinase interacting with the V3 loop of HIV-1 gp120 as cathepsin G. *FEBS Lett.* **345,** 81–6 (1994).

118. Coffey, M. J., Woffendin, C., Phare, S. M., Strieter, R. M. & Markovitz, D. M. RANTES inhibits HIV-1 replication in human peripheral blood monocytes and alveolar macrophages. *Am. J. Physiol. Cell. Mol. Physiol.* **272,** L1025–L1029 (1997).

119. Shi, G. P. *et al.* Role for cathepsin F in invariant chain processing and major histocompatibility complex class II peptide loading by macrophages. *J. Exp. Med.* **191,** 1177–86 (2000).

120. Maddocks, S. *et al.* Gene expression in HIV-1/*Mycobacterium tuberculosis* co-infected macrophages is dominated by M. tuberculosis. *Tuberculosis* **89,** 285–293 (2009).

121. Furci, L., Schena, E., Miotto, P. & Cirillo, D. M. Alteration of human macrophages microRNA expression profile upon infection with *Mycobacterium tuberculosis*. *Int. J. Mycobacteriology* **2,** 128–134 (2013).

122. Bergsbaken, T., Fink, S. L. & Cookson, B. T. Pyroptosis: host cell death and inflammation. *Nat. Rev. Microbiol.* **7,** 99–109 (2009).

123. Simeone, R. *et al.* Phagosomal Rupture by *Mycobacterium tuberculosis* Results in Toxicity and Host Cell Death. *PLoS Pathog.* **8,** e1002507 (2012).

124. Chen, K. L. *et al.* Targeting cathepsin S induces tumor cell autophagy via the EGFR-ERK signaling pathway. *Cancer Lett.* **317,** 89–98 (2012).

125. Pawar, K., Sharbati, J., Einspanier, R. & Sharbati, S. *Mycobacterium bovis* BCG Interferes with miR-3619-5p Control of Cathepsin S in the Process of Autophagy. *Front. Cell. Infect. Microbiol.* **6,** 27 (2016).

126. Pan, L. *et al.* Cathepsin S Deficiency Results in Abnormal Accumulation of Autophagosomes in Macrophages and Enhances Ang II–Induced Cardiac Inflammation. *PLoS One* **7,** e35315 (2012).

127. Pai, R. K., Convery, M., Hamilton, T. A., Boom, W. H. & Harding, C. V. Inhibition of IFN- -Induced Class II Transactivator Expression by a 19-kDa Lipoprotein from *Mycobacterium tuberculosis*: A Potential Mechanism for Immune Evasion. *J. Immunol.* **171,** 175–184 (2003).

128. Sendide, K. *et al.* Mycobacterium bovis BCG Attenuates Surface Expression of Mature Class II Molecules through IL-10-Dependent Inhibition of Cathepsin S. *J. Immunol.* **175,** 5324–5332 (2005).

129. Baena, A. & Porcelli, S. A. Evasion and subversion of antigen presentation by *Mycobacterium tuberculosis*. *Tissue Antigens* **74,** 189–204 (2009).

130. Sengupta, S. *et al. Mycobacterium tuberculosis* EsxL inhibits MHC-II expression by promoting hypermethylation in class-II transactivator loci in macrophages. *J. Biol. Chem.* **292,** 6855–6868 (2017).

131. Campbell-Yesufu, O. T. & Gandhi, R. T. Update on human immunodeficiency virus (HIV)-2 infection. *Clin. Infect. Dis.* **52,** 780–7 (2011).

132. Meng, Q.-L. *et al.* Identification of latent tuberculosis infection-related microRNAs in human U937 macrophages expressing *Mycobacterium tuberculosis* Hsp16.3. *BMC Microbiol.* **14,** 37 (2014).

List of Tables and Figures

List of acronyms

AIDS	acquired immunodeficiency syndrome
bp	base pairs
CTS	cathepsin
CST	cystatin
DC	dendritic cells
DR	death receptor
DNA	deoxyribonucleic acid
FasL	Fas ligand
FasR	Fas receptor
FcγR	Fcγ receptor
GFP	green fluorescent protein
GM-CSF	granulocyte macrophage colony-stimulating factor
HIV	human immunodeficiency virus
HLA	human leucocyte antigen
IFN	interferon
IL	interleukin
LAM	lipoarabinomannan
LTR	long terminal repeat
LPS	lipopolysaccharide
M-CSF	macrophage colony-stimulating factor
Mϕ	macrophages
MDM	monocyte-derived macrophages
MHC	major histocompatibility complex
MIP	macrophage inflammatory protein
miRNA	microRNA
Mtb	*Mycobacterium tuberculosis*
MOI	multiplicity of infection
Msm	*Mycobacterium smegmatis*
Ni	non-infected
NOS	nitrogen oxygen species
PBMC	peripheral blood mononuclear cell
PCR	polymerase chain reaction
Rab	Ras-related protein

ROS	reactive oxygen species
RNA	ribonucleic acid
RT	reverse transcriptase
TB	tuberculosis
THP-1	human leukaemia monocytic cell line
TLR	toll-like receptor
TNF	tumour necrosis factor
TNFR	tumour necrosis factor receptor
TRAIL	TNF-related apoptosis-inducing ligand

Annex

Annex Table 1: Primers used in the real time reverse transcriptase PCR.

Target Gene		Primer sequence (5'-3')
Cathepsin A	forward	CCACCTACCTCAACAACCCG
	reverse	GGATCTGGTATTTCTGTGAGCTA
Cathepsin B	forward	GGACAAGCACTACGGATACAAT
	reverse	CCGGTGACGTGTTGGTACA
Cathepsin C	forward	AACTGCTCGGTTATGGGACC
	reverse	ACCCACCCAGTCATTGTCTC
Cathepsin D	forward	CTCGTCAGGATCCCGCT
	reverse	CGATGCCAATCTCCCCGTAG
Cathepsin E	forward	ACTTGACATCCACCCTCCAG
	reverse	GAATGCCCCAGCCTAACATA
Cathepsin F	forward	TTGCCCTCCAATGCCTACTC
	reverse	GCCAGCTTCTGCTCGTTCT
Cathepsin G	forward	CTGAGGCAGGGGAGATCAT
	reverse	TGGGTGTTTTCCCGTCTCTG
Cathepsin H	forward	TGTCTAAGCACCGTAAGACCT
	reverse	GTCTGAAAATTGGTTCAGTGCCA
Cathepsin K	forward	CCGAAACGAAGCCAGACAAC
	reverse	GCCGAGAGATTTCATCCACCTTG
Cathepsin L	forward	GGCAACAGAAGAATCCTGTAAG
	reverse	CACTGCTACAGTCTGGCTCAA
Cathepsin O	forward	TTGATAAAACAGGAAGCACTCCA
	reverse	GCTGTCTCTTGATCTGCCCAA
Cathepsin S	forward	ATCACCACTGGCATCTCTGG
	reverse	ACTTCTTCACTGGTCATGTCTCC
Cathepsin V	forward	TCCGTGAGCCTCTGTTTCTT
	reverse	CTAGCCATGAAGCCACCATT
Cathepsin W	forward	CCACCCCAAGAAGTACCAGA
	reverse	GTGGCCTTGATCACACCTTT
Cathepsin Z	forward	GGGAGAAGATGATGGCAGAA
	reverse	ATAGGTGCTGGTCACGATCC
Cystatin A	forward	AAACCCGCCACTCCAGAAAT
	reverse	TTATCACCTGCTCGTACCTTAAT
Cystatin B	forward	TGTCATTCAAGAGCCAGGTG
	reverse	AGCTCATCATGCTTGGCTTT
Cystatin C	forward	CAACAAAGCCAGCAACGACAT
	reverse	AGAGCAGAATGCTTTCCTTTTCAGA
Cystatin D	forward	GATGAGTACTACAGCCGCCC
	reverse	AGCAGAACTCTTCCTCTTTCAGT
Cystatin E/M	forward	TCCGAGACACGCACATCATC
	reverse	TCACAGCGCAGCTTCTCCT
Cystatin F	forward	TCCCCAGATACTTGTTCCCAGG
	reverse	TTCTGCCAATTTCCACCTCCA

Cystatin S	forward	GCTCCAGCTTTGTGCTCTGCCT
	reverse	GTCTGCTCCCTGGCTCGCAG
Cystatin SA	forward	CTGCGGGTGCTACGAGCCAG
	reverse	GGAGGGAGGGCAGAGTCCCC
Cystatin SN	forward	TCCCTGCCTCGGGCTCTCAC
	reverse	ACCCGCAGCGGACGTCTGTA
GAPDH	forward	AAGGTGAAGGTCGGAGTCAA
	reverse	AATGAAGGGGTCATTGATGG

Annex Table 2: Reverse transcriptase activity in the supernatant of non-infected and infected macrophages, dendritic cells and peripheral blood mononuclear cells. Concentration of reverse transcriptase (RT) in samples was extrapolated from a linear regression line constructed with standard dilution of known concentration. Values presented are the average of biological triplicates. PBMC were used as positive control.

	RT ng/mL		
Sample	**Mϕ**	**DC**	**PBMC**
Ni	0.0	0.0	0.0
HIV-1	0.0	0.002	0.148
HIV-2	0.0	0.0	0.004
HIV-1 Msm	0.0	0.002	-
HIV-1 Mtb	0.0	0.004	-
HIV-2 Msm	0.0	0.0	-
HIV-2 Mtb	0.0	0.0	-

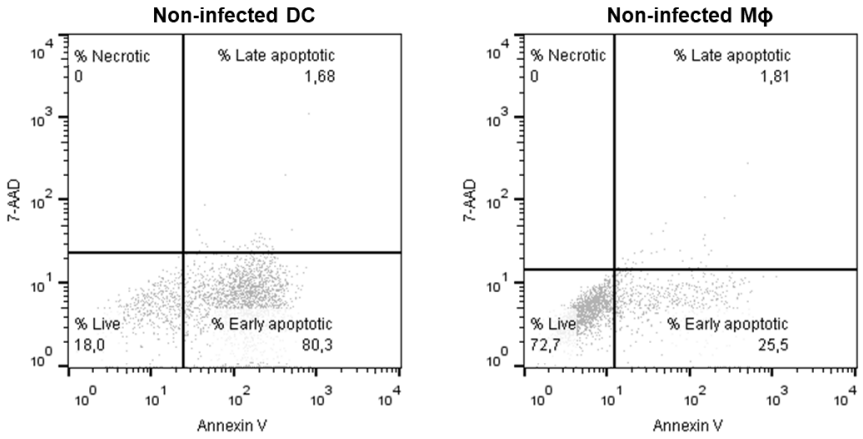

Annex Figure 1: Percentage of live, apoptotic and necrotic cells of non-infected dendritic cells and macrophages. The percentage of cells in each cellular stage is shown in the respective quadrant of the dot plot. Live cells (annexin V^-/7-AAD^-), early apoptotic cells (annexin V^+/7-AAD^-), late apoptotic cells (annexin V^+/7-AAD^+) and dead cells (annexin V^-/7-AAD^+). These graphs show the biological replicate that better

represents the average of the percentage of annexin V and 7-AAD positive cells (n = 3).

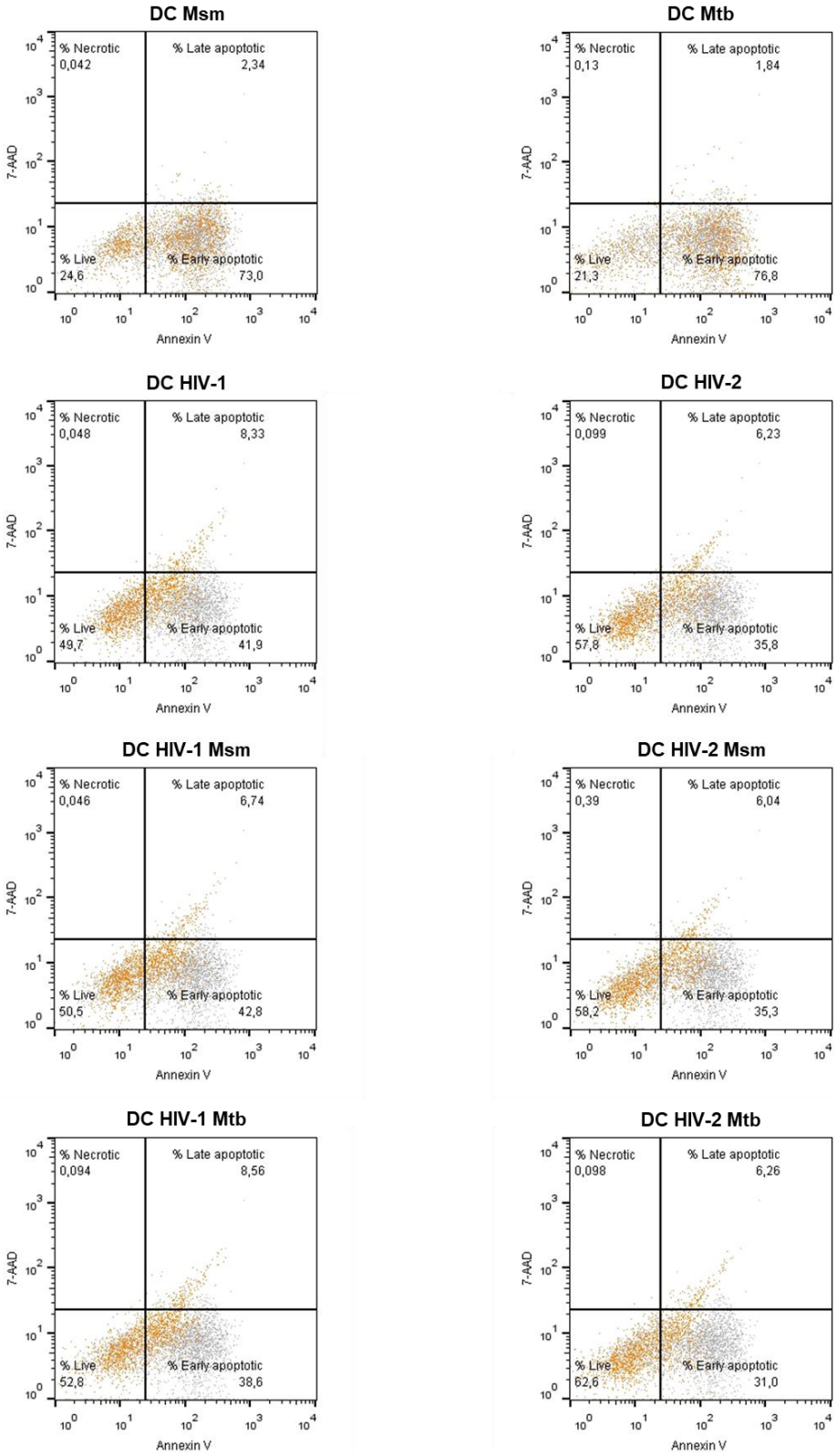

Annex Figure 2: Percentage of live, apoptotic and necrotic dendritic cells. Non-infected cells are presented in grey and infected cells in orange. The percentage of cells in each cellular stage is shown in the respective quadrant of the dot plot. Live cells (annexin V^- /7-AAD^-), early apoptotic cells (annexin V^+/7-AAD^-), late apoptotic cells (annexin V^+/7-

AAD$^+$) and dead cells (annexin V$^-$/7-AAD$^+$). These graphs show the biological replicate that better represents the average of the percentage of annexin V and 7-AAD positive cells (n = 3).

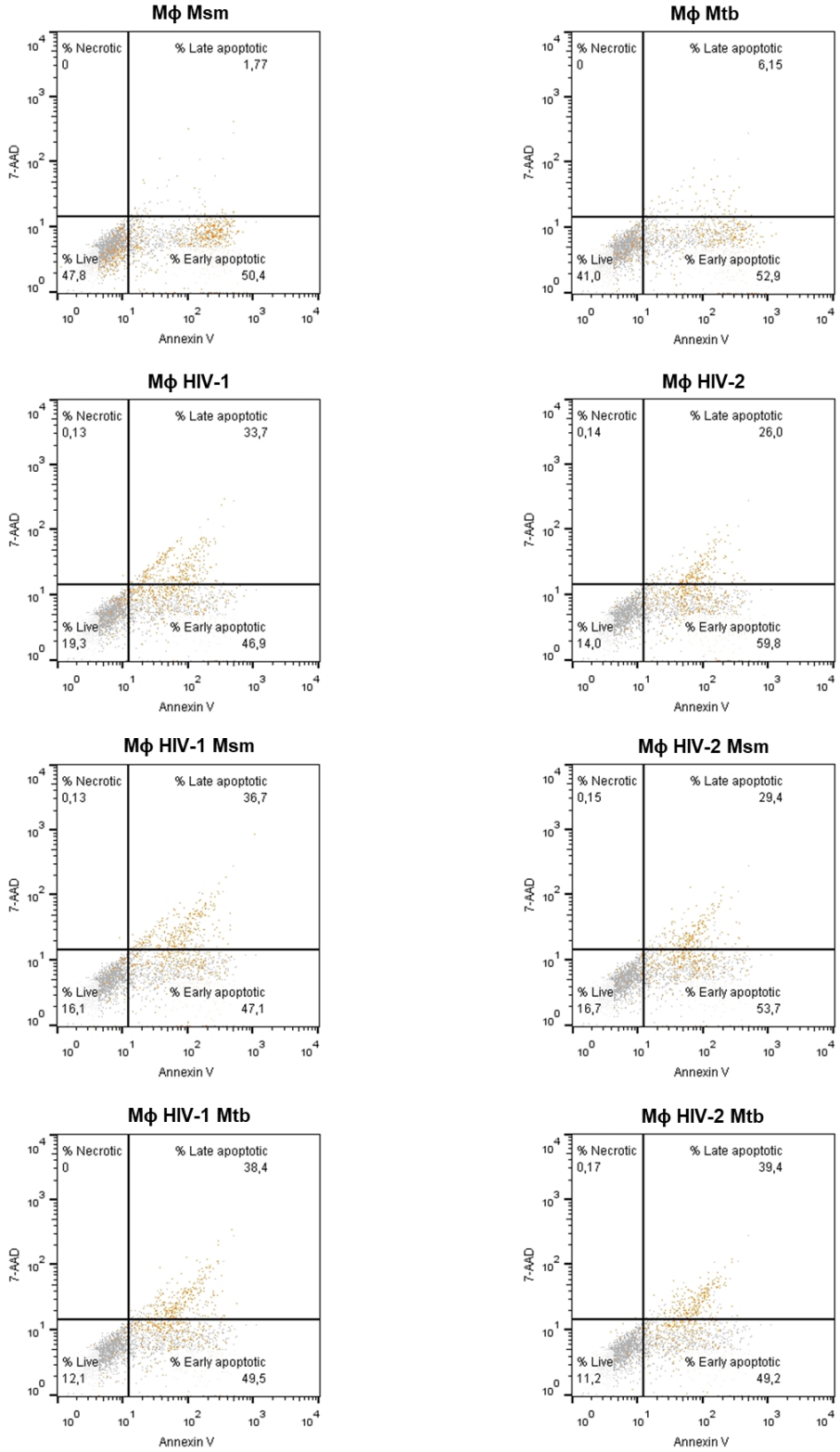

Annex Figure 3: Percentage of live, apoptotic and necrotic macrophages. Non-infected cells are presented in grey and infected cells in orange. The percentage of cells in each cellular stage is shown in the respective quadrant of the dot plot. Live cells (annexin V$^-$ /7-AAD$^-$), early apoptotic cells (annexin V$^+$/7-AAD$^-$), late apoptotic cells (annexin V$^+$/7-

AAD$^+$) and dead cells (annexin V$^-$/7-AAD$^+$). These graphs show the biological replicate that better represents the average of the percentage of annexin V and 7-AAD positive cells (n = 3).